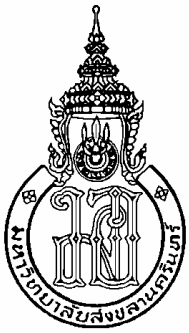

Adsorption of Rhodamine B on Commercial Activated Carbon and Activated Carbon Obtained from Pericarp of Rubber Fruit

Fareeda Hayeeye

A Thesis Submitted in Partial Fulfillment of the Requirements for the Degree of Master of Science in Physical Chemistry

Prince of Songkla University

2010

Thesis Title	Adsorption of Rhodamine B on Commercial Activated Carbon and Activated Carbon Obtained from Pericarp of Rubber Fruit
Author	Miss Fareeda Hayeeye
Major Program	Physical Chemistry

Major Advisor:

……
(Asst. Prof. Dr. Orawan Sirichote)

Co-advisor:

……
(Asst. Prof. Dr. Surajit Tekasakul)

Examining Committee:

…….Chairperson
(Asst. Prof. Dr. Usa Onthong)

…….....
(Asst. Prof. Dr. Orawan Sirichote)

…….
(Asst. Prof. Dr. Surajit Tekasakul)

…….
(Asst. Prof. Dr. Chaveng Pakawatchai)

The Graduate School, Prince of Songkla University, has approved this thesis as partial fulfillment of the requirements for the Master of Science Degree in Physical Chemistry.

……
(Prof. Dr. Amornrat Phongdara)
Dean of Graduate School

ชื่อวิทยานิพนธ์ การดูดซับสีย้อม Rhodamine B บนถ่านกัมมันต์ทางการค้าและถ่านกัมมันต์ที่เตรียมจากเปลือกลูกยาง

ผู้เขียน นางสาวฟารีดา หะยีเย๊ะ

สาขาวิชา เคมีเชิงฟิสิกส์

ปีการศึกษา 2553

บทคัดย่อ

ศึกษาลักษณะเฉพาะทางกายภาพของถ่านกัมมันต์ทางการค้า (CAC) และถ่านกัมมันต์ที่เตรียมจากเปลือกลูกยาง (PrAC) และการดูดซับสารละลายสีย้อม Rhodamine B บน CAC และ PrAC ปัจจัยที่ใช้ในการดูดซับ คือ เวลาที่เข้าสู่สมดุลของการดูดซับ ความเข้มข้นเริ่มต้นของสารละลายสีย้อม Rhodamine B ปริมาณตัวดูดซับ pH และอุณหภูมิ จากผลการทดลองพบว่ารูปแบบการดูดซับของถ่านกัมมันต์ทั้งสองชนิดสอดคล้องกับสมการของ Langmuir isotherm โดยปริมาณการดูดซับสีย้อม Rhodamine B สูงสุด (Q_m) บน CAC คือ 0.90, 0.96, 0.98 และ 1.03 mmol g^{-1} และปริมาณการดูดซับสีย้อม Rhodamine B สูงสุด (Q_m) บน PrAC คือ 0.23, 0.24, 0.28 และ 0.30 mmol g^{-1} ที่อุณหภูมิ 30, 40, 50 และ 60 °C ตามลำดับ และจากข้อมูลทางเทอร์โมไดนามิกส์ค่าเอนทัลปีของการดูดซับ (H_{ads}) มีค่าเป็นบวกแสดงให้เห็นว่าการดูดซับที่เกิดขึ้นเป็นกระบวนการแบบดูดความร้อนและจากค่า Seperation factor (R_L) ซึ่งมีค่าในช่วง $0 < R_L < 1$ แสดงว่าการดูดซับเกิดขึ้นได้ดี อีกทั้ง PrAC ดูดซับสารละลายสีย้อม Rhodamine B ได้ประมาณ 80 – 90% จึงสามารถนำถ่านกัมมันต์จากเปลือกลูกยาง (PrAC) ที่เตรียมจากวัสดุทางการเกษตรมาใช้แทนถ่านกัมมันต์ทางการค้า (CAC) ได้

Thesis Title	Adsorption of Rhodamine B on Commercial Activated Carbon and Activated Carbon Obtained from Pericarp of Rubber Fruit
Author	Miss Fareeda Hayeeye
Major Program	Physical Chemistry
Academic Year	2553

ABSTRACT

A commercial activated carbon (CAC) and activated carbon obtained from pericarp rubber fruit (PrAC) were characterized for some physical properties and tested for their efficiency in adsorption of Rhodamine B. The parameters affect the adsorption had been studied such as contact time, initial dye concentration, weight of activated carbon, pH and temperature. Langmuir isotherm model was applied to the equilibrium data. The maximum adsorption (Q_m) obtained from the Langmuir isotherm plots were 0.90, 0.96, 0.98, and 1.03 mmol g^{-1} for CAC, and 0.23, 0.24, 0.28, and 0.30 mmol g^{-1} for PrAC at 30, 40, 50, and 60°C, respectively. The positive values of the heat of adsorption (H_{ads}) indicate the endothermic nature of adsorption. The range of dimensionless seperation factor (R_L) values is $0 < R_L < 1$ indicating that the adsorption is favorable. The adsorption efficiency of Rhodamine B on PrAC is about 80-90%. Therefore, PrAC which is agricultural product can be used in place of commercial activated carbon for removal of dyes from waste.

ACKNOWLEDGEMENTS

I would like to express my sincere thanks to my advisor, Assistant Professor Dr. Orawan Sirichote, who suggested this research problem, for her numerous comments, encouragement, criticism and kindness during the laboratory work and the preparation of this thesis.

I am grateful to my co-advisor, Assistant Professor Dr. Surajit Tekasakul, who has given her time in reviewing the text and suggested the improvement of the report. I am also grateful to Assistant Professor Dr. Chaveng Pakawatchai and Assistant Professor Dr. Usa Onthong, the examining chairperson for their kind comments and correction of this thesis. I would like to thank to Mr. Sathorn Panumati, who gave the valuable suggestion for this research.

I would like to thank the staff of the Department of Chemistry and also too many other people for their help and encouragement during my study.

I am grateful to the Department of Chemistry, Faculty of Science, Prince of Songkla University, Hat Yai; the Center of Excellence for Innovation in Chemistry: Postgraduate Education and Research Program in Chemistry (PERCH – CIC) Commission on Higher Education, Ministry of Education, and the Graduate School, Prince of Songkla University for their partially supported.

Love, encouragement from my family and friends will be remembered.

Fareeda Hayeeye

CONTENTS

CONTENTS (Continued)

Page

LIST OF TABLES

PrAC (0.09 g), pH = 4.

LIST OF FIGURES

LIST OF FIGURES (Continued)

CHAPTER 1

INTRODUCTION

1.1 Introduction

Waste water including waste water from manufacturing processes, buildings, residences, and shops which may bring some substances such as organic substances, inorganic substances, acid alkaline, heavy metals, some chemical substances, radioactivity substances, toxic substances, sandy soil, and other wastes. When these wastes are thrown into the river, the quantity of those substances will be increased or will become toxicity for living things in the water. Most of contaminants in waste water caused by dye in dye industry are dyes and chemical substances which is the left over part in the water using in manufacturing process and being thrown into the waste water. Although there are some arguments that dye should not grouping to one of the substances caused to water pollution, due to the disgusted feeling of ordinary people, the ministry of industrial's declaration about the standard of waste water from the industry has been determined that the color of waste water is not disgusted. Thus, before waste water from the dye industry will be released from the industry, the waste water curing system has to be done for destroying some substances including the left over color. There are many methods to destroy the color but one of the interesting ways is adsorption by using activated carbon. This method is efficient for dye adsorption since the efficiency of dye adsorption will be increased with increasing pore distributions.

Most dye-containing effluents from various industrial branches, mainly dye manufacturing and textile finishing, are discharged into river streams. Even in low concentrations, dyes affect aquatic life and the food web. Because many organic dyes are harmful to human beings, the removal of color from process or waste effluents is environmentally important. Rhodamine B was selected for the adsorption experiment due to its presence in the wastewaters of several industries (such as textile, leather, jute and food industries). Wastewaters from dyeing industries released into nearby

land or rivers without any treatment because the ordinary treatment methods have to spend the high cost for being effective. Hence adsorption is one of the most effective methods and activated carbon is the preferred adsorbent widely employed to treat wastewater containing different classes of dye. The reason why we usually use this method is that it is able to use the various kinds of waste to prepare the activated carbons.

1.2 Preliminary knowledge and theoretical section

1.2.1 Definition of activated carbon

Activated carbon, also called activated charcoal or activated coal is a form of carbon that has been processed to make it extremely porous and thus to have a very large surface area available for adsorption or chemical reactions.

The word *activated* in the name is sometimes replaced with *active*. Due to its high degree of microporosity, just one gram of activated carbon has a surface area in excess of 500 m^2, as determined typically by nitrogen gas adsorption. Sufficient activation for useful applications may come solely from the high surface area, though further chemical treatment often enhances the adsorbing properties of the material.

Activated carbon mainly consists of elementary carbon in graphite alike structure. It can be produced by heat treatment, or “activation”, of raw materials such as wood, coal, peat and coconut shell. During the activation process, the unique internal pore structure is created, and it is this pore structure which provides activated carbon its outstanding adsorption properties.

Activated carbons are complex products which are difficult to classify on the basis of their behaviors, surface characteristics and preparation methods. However, some broad classification is made for general purpose based on their physical characteristics (Chuenchom, 2004).

Classification

(1) Powdered activated carbon (PAC)

Traditionally, active carbons are made in particular form as powders or fine granules less than 1.0 mm in size with an average diameter between 0.15 and 0.25 mm. Thus they present a large surface to volume ratio with a small diffusion distance. PAC is made up of crushed or ground carbon particles, 95–100% of which will pass through a designated mesh sieve or sieve. Granular activated carbon is defined as the activated carbon being retained on a 50 mesh sieve (0.297 mm) and PAC material as finer material, while ASTM classifies particle sizes corresponding to an 80 mesh sieve (0.177 mm) and smaller as PAC. PAC is generally added directly to other process units, such as raw water intakes, rapid mix basins, clarifiers, and gravity filters. In this research, particle sizes of both activated carbons 200 – 270 mesh sieve which are PAC.

(2) Granular activated carbon (GAC)

Granular activated carbon are irregular shaped particles with sizes ranging from 0.2 to 5 mm which has a relatively larger particle size compared to powdered activated carbon and consequently, presents a smaller external surface. Granulated carbons are used for water treatment, deodorization and separation of components of flow system. This type is used in both liquid and gas phase applications.

(3) Extruded activated carbon (EAC)

Extruded activated carbon combines powdered activated carbon with a binder, which are fused together and extruded into a cylindrical shaped activated carbon block with diameters from 0.8 to 130 mm. These are mainly used for gas phase applications because of their low pressure drop, high mechanical strength and low dust content.

(4) Impregnated carbon

Porous carbons containing several types of inorganic impregnant such as iodine, silver, cation such as Al, Mn, Zn, Fe, Li, Ca have also been prepared for specific application in air pollution control especially in museums and galleries. Due

to antimicrobial/antiseptic properties, silver loaded activated carbon is used as an adsorbent for purifications of domestic water. Drinking water can be obtained from natural water by treating the natural water with a mixture of activated carbon and flocculating agent $Al(OH)_3$. Impregnated carbons are also used for the adsorption of H_2S and thiols (mercaptans). Adsorption rates for H_2S as high as 50% by weight have been reported.

(5) Polymers coated carbon

This is a process by which a porous carbon can be coated with a biocompatible polymer to give a smooth and permeable coat without blocking the pores. The resulting carbon is useful for hemoperfusion. Hemoperfusion is a treatment technique in which large volumes of the patient's blood are passed over an adsorbent substance in order to remove toxic substances from the blood.
(http://en.wikipedia.org/wiki/Activated carbon**)**

Utilities of activated carbon

Activated carbon, the common factor in hundreds of different applications just a grab from the numerous applications: decolourisation of sugar and sweeteners, drinking water treatment, gold recovery, production of pharmaceuticals and fine chemicals, catalytic processes, off gas treatment of waste incinerators, automotive vapour filters, colour/odour correction in wines and fruit juices, additive in liquorice, etc.

In its numerous applications, activated carbon represents a number of different functionalities:

Adsorption: the most well-known mechanism, through chemisorption or physical adsorption (Van der Waals forces)

Reduction: e.g. removal of chlorine from water is based on chemical reduction reactions.

Catalysis: activated carbon can catalyse a number of chemical conversions, or can be a carrier of catalytic agents (e.g. precious metals).

Carrier of biomass: supported material in biological filters.

Carrier of chemicals: e.g. slow release applications colourant, activated carbon's function in decolourizing (Chuenchom, 2004).

1.2.2 The activation process of activated carbon

Activation refers to the development of the adsorption properties of carbon. It can be produced by one of the following processes:

(1) Physical activation: The precursor is developed into activated carbons using gases. This is generally done by using one or a combination of the following processes:

Carbonization: Material with carbon content is pyrolyzed at temperatures in the range 600–900 °C, in absence of air (usually in inert atmosphere with gases like argon or nitrogen)

Activation/Oxidation: Raw material or carbonized material is exposed to oxidizing atmospheres (carbon dioxide, oxygen, or steam) at temperatures above 250 °C, usually in the temperature range of 600–1200 °C.

(2) Chemical activation: One of the key steps in the production of activated carbon is chemical activation through the impregnation of the raw material with chemicals such as phosphoric acid, potassium hydroxide, zinc chloride. These additives are known to enhance carbonization, resulting in improved development of the pore structure. Chemical activation is usually limited to woody precursors. Among the activating agent used for the production of activated carbon from carbonaceous material, zinc chloride has been proven to be one of the most effective impregnants. Zinc chloride acts as a dehydration agent, influencing the decomposition of carbonaceous material during the pyrolysis, thus restricting the formation of tar and increasing the carbon yield. The degradation of cellulose material and the aromatization of the carbon skeleton upon zinc chloride treatment result in the creation of the pore structure. These pores are the interstices left vacant upon the removal of zinc chloride from the carbon matrix by intensive washing. The studies have clearly demonstrated that the amount of zinc chloride used during chemical activation significantly impacts the

structure characteristics of the carbons (http://en.wikipedia.org/wiki/Activated carbon).

1.2.3 Porosity: definition

Based on the experience of adsorption chemistry, total porosity is classified into three groups. The origins and structure of porosities are elaborated upon below. IUPAC classifies porosities as follows:

- Micropores width less than 2 nm
- Mesopores width between 2 and 50 nm
- Macropores width greater than 50 nm

It has also been useful to classify micropores further into ultra-(< 0.5 nm width) and super- (1.0 – 2.0 nm) micropores, these definitions being relevant when considering adsorption behavior. Micropores are considered as being about the size of adsorbate molecules and accommodate one, two or perhaps three molecules. Mesoporosity is wider than micropores. Macroporosity has little interest for the surface chemist. They are transport pores to the interior of particles and are considered as external surface. Some activate carbons contain all of these sizes of porosity associated with the botanical composition of the material. The pore size distribution is highly important for the practical application; the best fit depends on the compounds of interest, the matrix (gas, liquid) and treatment condition. The desired pore structure of an activated carbon product is attained by combining the right raw material and activation conditions (Chuenchom, 2004).

1.2.4 Evolution of Dyes

The preparation and application of dyestuffs are the oldest forms of human activities. Evidences of which were found by excavation at archaeological sites where ancient fabrics were unearthed. There is also mention of it in the Bible and other works of classical antiquity. It was in 2600 BC when earliest written records of the use of dyestuffs were found in China. Perhaps one of the real breakthroughs in the history of dyes came in 1856 when a teenager who was experimenting at his makeshift laboratory in home made a certain discovery that acted as a sort of the modern chemicals industry.

William Perkin an 18-year-old student was working on chemical synthesis of natural products. In a classic case of serendipity, the young William Perkin chanced upon his now famous 'Aniline Mauve' dyes while he was attempting to synthesize quinine, the only cure for malaria. Perkin named his color Mauveine, after the French name of non-fast color which was made of natural dyes. So "Mauve" (a basic dye) was the first synthetic dye stuff. Mauve was a derivative of coal tar. It was the first mass-produced dye, that was commercially available and the idea was born that a color could be made in the factory. It was indeed a revolution.

This is a very common question that occurs in everybody mind. The answer to which is explained by the presence of a substance called *Chromophore* in the dyes. By definition dyes are basically aromatic compounds. Their structures have aryl rings that has delocalised electron systems. These structures are said to be responsible for the absorption of electromagnetic radiation that has varying wavelengths, based upon the energy of the electron clouds. It is actually because of this reason that chromophores do not make dyes coloured. Rather it makes the dyes proficient in their ability to absorb radiation. Chromophores acts by making energy changes in the delocalised electron cloud of the dye. This alteration invariably results in the compound absorbing radiation within the visible range of colours and not outside it. Human eyes detect this absorption, and responds to the colours.

Another possibility is that if the electrons are removed from the electron cloud, it may result in loss of color. Removing electrons may cause the rest of the electrons to revert to the local orbits. A very good example is the Schiff's reagent. As sulphurous acid reacts with pararosanilin, what happens is that a sulphonic group attaches itself to the compound's central carbon atom. This hampers the conjugated double bond system of the quinoid ring, and causes the electrons to become localised. As a consequence the ring ceases to be a chromophore. As a result, the dye becomes colourless.

To conclude chromophores are the atomic configurations which has delocalised electrons. Generally they are represented as carbon, nitrogen, oxygen and sulphur. They can have alternate single and double bonds.

Classification of dyes

The first human-made (synthetic) organic dye, mauveine was discovered by William Henry Perkin in 1856. Many thousands of synthetic dyes have since been prepared.

Synthetic dyes quickly replaced the traditional natural dyes. They cost less, they offered a vast range of new colors, and they imparted better properties to the dyed materials. Dyes are now classified according to how they are used in the dyeing process.

(1) Acid dyes are water-soluble anionic dyes that are applied to fibers such as silk, wool, nylon and modified acrylic fibers using neutral to acid dye baths. Attachment to the fiber is attributed, at least partly, to salt formation between anionic groups in the dyes and cationic groups in the fiber. Acid dyes are not substantive to cellulose fibers. Most synthetic food colors fall in this category.

(2) Basic dyes are water-soluble cationic dyes that are mainly applied to acrylic fibers, but find some use for wool and silk. Usually acetic acid is added to the dye bath to help the uptake of the dye onto the fiber. Basic dyes are also used in the coloration of paper.

(3) Direct or **substantive dyeing** is normally carried out in a neutral or slightly alkaline dyebath, at or near boiling point, with the addition of either sodium chloride (NaCl) or sodium sulfate (Na_2SO_4). Direct dyes are used on cotton, paper, leather, wool, silk and nylon. They are also used as pH indicators and as biological stains.

(4) Mordant dyes require a mordant, which improves the fastness of the dye against water, light and perspiration. The choice of mordant is very important as different mordants can change the final color significantly. Most natural dyes are mordant dyes and there is therefore a large literature base describing dyeing techniques. The most important mordant dyes are the synthetic mordant dyes, or chrome dyes, used for wool; these comprise some 30% of dyes used for wool, and are especially useful for black and navy shades. The mordant, potassium dichromate, is applied as an after-treatment. It is important to note that many mordants, particularly those in the heavy metal category, can be hazardous to health and extreme care must be taken in using them.

(5) Vat dyes are essentially insoluble in water and incapable of dyeing fibers directly. However, reduction in alkaline liquor produces the water soluble alkali metal salt of the dye, which, in this leuco form, has an affinity for the textile fiber. Subsequent oxidation reforms the original insoluble dye. The color of denim is due to indigo, the original vat dye.

(6) Reactive dyes utilize a chromophore attached to a substituent that is capable of directly reacting with the fibre substrate. The covalent bonds that attach reactive dye to natural fibers make them among the most permanent of dyes. "Cold" reactive dyes, such as Procion MX, Cibacron F, and Drimarene K, are very easy to use because the dye can be applied at room temperature. Reactive dyes are by far the best choice for dyeing cotton and other cellulose fibers at home or in the art studio.

(7) Disperse dyes were originally developed for the dyeing of cellulose acetate, and are water insoluble. The dyes are finely ground in the presence of a dispersing agent and sold as a paste, or spray-dried and sold as a powder. Their main use is to dye polyester but they can also be used to dye nylon, cellulose triacetate, and acrylic fibres. In some cases, a dyeing temperature of 130 °C is required, and a pressurised dyebath is used. The very fine particle size gives a large surface area that aids dissolution to allow uptake by the fibre. The dyeing rate can be significantly influenced by the choice of dispersing agent used during the grinding.

(8) Azoic dyeing is a technique in which an insoluble azo dye is produced directly onto or within the fibre. This is achieved by treating a fibre with both diazoic and coupling components. With suitable adjustment of dyebath conditions the two components react to produce the required insoluble azo dye. This technique of dyeing is unique, in that the final color is controlled by the choice of the diazoic and coupling components.

(9) Sulfur dyes are two parts "developed" dyes used to dye cotton with dark colors. The initial bath imparts a yellow or pale chartreuse color; this is aftertreated with a sulfur compound in place to produce the dark black we are familiar with in socks for instance. Sulfur Black 1 is the largest selling dye by volume.
(http://en.wikipedia.org/wiki/dye)

1.2.5 Rhodamine

Rhodamine is a family of related chemical compounds, fluorone dyes. Examples are Rhodamine 6G and Rhodamine B. They are used as a dye and as a dye laser gain medium. It is often used as a tracer dye within water to determine the rate and direction of flow and transport. Rhodamine dyes fluoresce and can thus be detected easily and inexpensively with instruments called fluorometers. Rhodamine dyes are used extensively in biotechnology applications such as fluorescence microscopy, flow cytometry, fluorescence correlation spectroscopy and Enzyme-linked immunosorbent assay (ELISA). Rhodamine dyes are generally toxic, and are soluble in water, methanol and ethanol.

The structure of Rhodamine B in aqueous solution is displayed below.

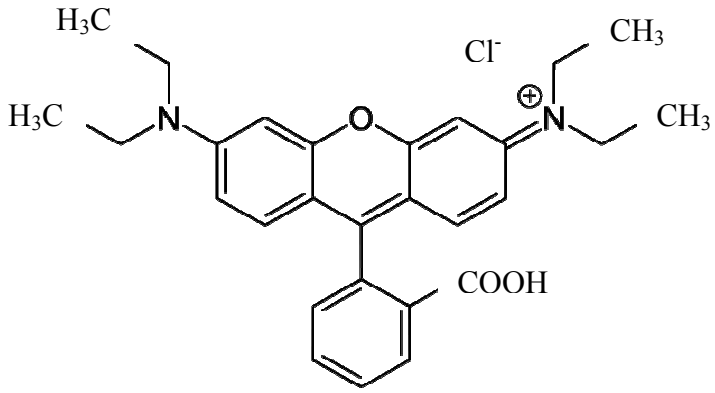

Figure 1 Structure of Rhodamine B.

IUPAC name: [9-(2-carboxyphenyl)-6-diethylamino-3-xanthenylidene]-diethylammonium chloride

Other names: Rhodamine 610, C.I. Pigment Violet 1, Basic Violet 10, C.I. 45170

Characteristics of Rhodamin B

Molecular formula: $C_{28}H_{31}ClN_2O_3$

Molar mass: 479.02

Appearance: red to violet

Melting point: 210 - 211 °C (Decomposes)

Classification of dye: basic dye

Rhodamine B is often used as a tracer dye within water to determine the rate and direction of flow and transport. Rhodamine B is used in biology as a staining fluorescent dye, sometimes in combination with auramine O, as the auramine-rhodamine stain to demonstrate acid-fast organisms, notably Mycobacterium.

Solubility in water is ~50 g L^{-1}. However, the solubility in acetic acid solution (30 vol. %) is ~400 g L^{-1}. Chlorinated tap water decomposes Rhodamine B. Rhodamine B solutions adsorb to plastics and should be kept in glass.

Rhodamine B is being tested for use as a biomarker in oral rabies vaccines for wildlife, such as raccoons, to identify animals that have eaten vaccine bait.

1.2.6 Adsorption

Adsorption is the adhesion of molecules of gas, liquid, or dissolved solids to a surface. This process creates a film of the *adsorbate* (the molecules or atoms being accumulated) on the surface of the *adsorbent*. It differs from *absorption*, in which a fluid permeates or is dissolved by a liquid or solid. The term sorption encompasses both processes, while desorption is the reverse of adsorption.

Similar to surface tension, adsorption is a consequence of surface energy. In a bulk material, all the bonding requirements (be they ionic, covalent, or metallic) of the constituent atoms of the material are filled by other atoms in the material. However, atoms on the surface of the adsorbent are not wholly surrounded by other adsorbent atoms and therefore can attract adsorbates. The exact nature of the bonding depends on the details of the species involved, but the adsorption processes are two different types:

(1) Physisorption, where the adsobates were held by physical (i.e., Van der Waals) forces. These forces can be eliminated (removal of molecules from surface of adsorbent) when increasing temperature. Therefore, physisorption can be called reversible process.

(2) Chemisorption, where there is direct chemical bond between the adsorbate and the surface. This bond cannot be broken by only increased temperature. This behavior is usually irreversible process.

Chemisorption and physisorption are usually distinguishable from each other without any great difficulty. Table A summarizes the main criteria.

Table A Criteria for distinguishing between chemisorption and physisorption. (Bond, 1987)

Criteria	Chemisorption	Physisorption
Enthalpy of adsorption or heat of adsorption (H_{ads})	> 40 kJ/mol usually around 600-700 kJ/mol	0 – 40 kJ/mol
Activation energy, E_a	Usually small	Zero
Increasing temperature	Irreversible	Reversible

The adsorption characteristics in solution phase between the adsorbent and adsorbate were explained by the adsorption isotherm models in general. Several models can be used to describe adsorption data. The two most frequently used for dilute solutions are the Langmuir and Freundlich isotherms (Chuenchom, 2004).

Adsorption isotherm

The process of Adsorption is usually studied through graphs which are known as adsorption isotherm. It is the graph between the amounts of adsorbate (Q_e) adsorbed on the surface of adsorbent (m) and pressure at constant temperature. Different adsorption isotherms have been Freundlich, Langmuir and BET theory.

Basic adsorption isotherm

In the process of adsorption, adsorbate gets adsorbed on adsorbent.

$$\text{Adsorbate} + \text{Adsorbent} \underset{\text{Desorption}}{\overset{\text{Adsorption}}{\rightleftharpoons}} \text{Adsorption}$$

According to Le Chatelier principle, the direction of equilibrium would shift in that direction where the stress can be relieved. In case of application of excess of pressure to the equilibrium system, the equilibrium will shift in the direction where the number of molecules decreases. Since number of molecules decreases in forward

direction, with the increases in pressure, forward direction of equilibrium will be favored.

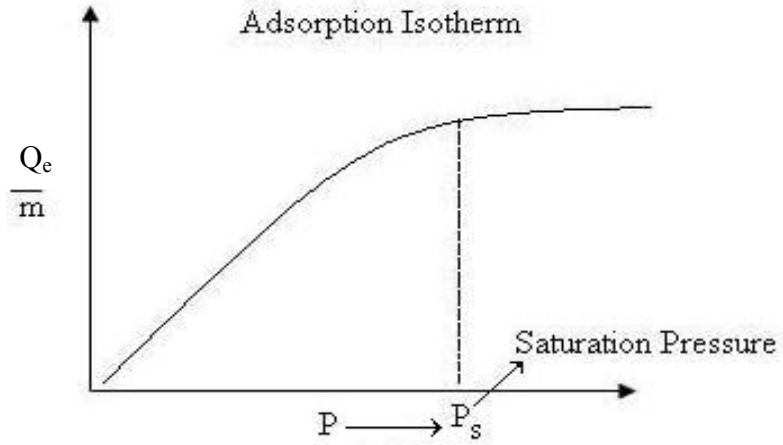

From the graph, we can predict that after saturation pressure P_s, adsorption does not occur anymore. This can be explained by the fact that there are limited numbers of vacancies on the surface of the adsorbent. At high pressure a stage is reached when all the sites are occupied and further increase in pressure does not cause any difference in adsorption process. At high pressure, adsorption is independent of pressure.

Langmuir adsorption isotherm

In 1916 Langmuir proposed another adsorption isotherm known as Langmuir adsorption isotherm. This isotherm was based on different assumptions one of which is that dynamic equilibrium exists between adsorbed gaseous molecules and the free gaseous molecules.

$$A(g) + B(S) \underset{\text{Desorption}}{\overset{\text{Adsorption}}{\rightleftharpoons}} AB$$

Where A (g) is unadsorbed gaseous molecule, B(s) is unoccupied surface and AB is adsorbed gaseous molecule.

Based on his theory, he derived Langmuir equation which depicted a relationship between the number of active sites of the surface undergoing adsorption and pressure.

$$Q_e \quad \frac{Q_m b C_e}{1 \quad b C_e} \qquad \text{(Nonlinear form)} \qquad (1)$$

Where Q_e represents the amount of solute adsorbed per unit weight of adsorbent (mmol g^{-1}); Q_m is the amount of solute adsorbed per unit weight of adsorbent required for monolayer coverage of the surface, also called the monolayer capacity (mmol g^{-1}); C_e is the concentration of adsorbate in solution at equilibrium conditions (mmol L^{-1}); and b is an equilibrium constant related to the heat of adsorption, $b \quad e^{(H_{ads} / RT)}$ (Adamson and Gast, 1997)

Equation (1) is usually linearlized by inversion to obtain the following from

$$\frac{C_e}{Q_e} \quad \frac{1}{bQ_m} \quad \frac{C_e}{Q_m} \qquad \text{(Linear form)} \qquad (2)$$

Many researchers have usually used equation (2) to analyse batch equilibrium data by plotting C_e / Q_e versus C_e, which yields a linear if data conform to the Langmuir isotherm (Arivoli, 2009).

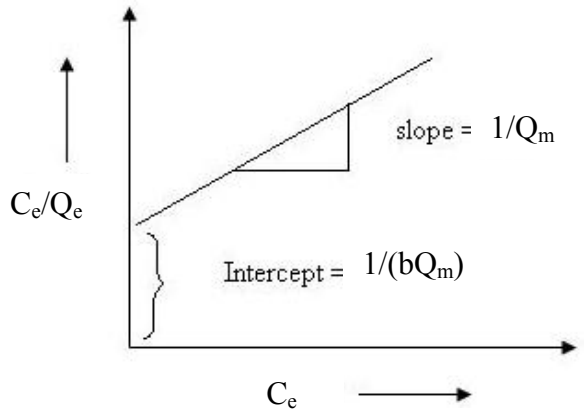

Once b is considered, this parameter can be rewritten as

$$b \quad b'e \quad ^{H_{ads} / RT} \qquad (3)$$

Where H_{ads} is enthalpy or heat of adsorption, R is the universal gas constant, T is the temperature in Kelvin and b' is pre- exponential factor constant.

The heat of adsorption (H_{ads}) can be determined from slope of the observed linearity from the plot of ln b (or log) versus 1/T that leads to heat process involved in adsorption at monolayer coverage.

Assumptions of Langmuir isotherm

Langmuir proposed his theory by making following assumptions.

1. Fixed number of vacant or adsorption sites are available on the surface of solid.
2. All the vacant sites are of equal size and shape on the surface of adsorbent.
3. Each site can hold maximum of one gaseous molecule and a constant amount of heat energy is released during this process.
4. Dynamic equilibrium exists between adsorbed gaseous molecules and the free gaseous molecules. $A(g) + B(S) \underset{\text{Desorption}}{\overset{\text{Adsorption}}{\rightleftharpoons}} AB$

Where A (g) is unadsorbed gaseous molecule, B(s) is unoccupied surface and AB is adsorbed gaseous molecule.

5. Adsorption is monolayer or unilayer.

Limitations of Langmuir adsorption equation

1. The adsorbed gas has to behave ideally in the vapor phase. This condition can be fulfilled at low pressure conditions only. Thus Langmuir equation is valid under low pressure only.
2. Langmuir equation assumes that adsorption is monolayer. But, monolayer formation is possible only under low pressure condition. Under high pressure condition the assumption breaks down as gas molecules attract more and more molecules towards each other. *BET theory* proposed by Brunauer, Emmett and Teller explained more realistic multilayer adsorption process.
3. Another assumption was that all the sites on the solid surface are equal in size and shape and have equal affinity for adsorbate molecules i.e. the surface of solid if homogeneous. But we all know that in real solid surfaces are heterogeneous.
4. Langmuir Equation assumed that molecules do not interact with each other. This is impossible as weak force of attraction exists even between molecules of same type.
5. The adsorbed molecules has to be localized i.e. decrease in randomness is zero ($\Delta S = 0$).This is not possible because on adsorption liquefaction of gases

taking place, which results into decrease in randomness but the value is not zero.

From above facts we can conclude that, Langmuir equation is valid under low pressure conditions**.**

Freundlich adsorption isotherm

Freundlich proposed another adsorption isotherm known as Freundlich adsorption isotherm or Freundlich adsorption equation or simply Freundlich isotherm. The Freundlich adsorption equation is perhaps the most widely used for the description of adsorption in aqueous systems. The Freundlich equation is of the form

$$Q_e \quad K_F C_e^{1/n} \qquad \text{(Non linear form)} \quad (4)$$

Where Q_e and C_e have definitions as previously presented for the Langmuir isotherm. K_F is the so-called unit capacity factor that shows adsorption capacity and n is the empirical parameter that represents the herogeneity of the site energies and also is indicative of the intensity of adsorption.

The logarithm of equation (4) given below is usually used to fit data as

$$\log Q_e \quad \log K_F \quad \frac{1}{n}\log C_e \qquad \text{(Linear form)} \quad (5)$$

The above equation is comparable with equation of straight line, y = mx + c where, m represents slope of the line and c represents intercept on y axis.

Plotting a graph between log Q_e and log C_e, we will get a straight line with value of slope equal to n and log K_F as y-axis intercept (Arivoli, 2009).

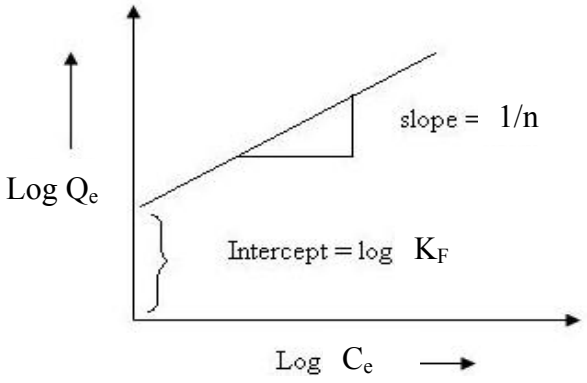

Limitation of Freundlich adsorption isotherm

Experimentally it was determined that extent of adsorption varies directly with pressure till saturation pressure P_s is reached. Beyond that point rate of adsorption saturates even after applying higher pressure. Thus Freundlich adsorption isotherm failed at higher pressure.

Type of adsorption isotherm

Five different types of adsorption isotherm and their characteristics are explained below.

Type I Adsorption isotherm

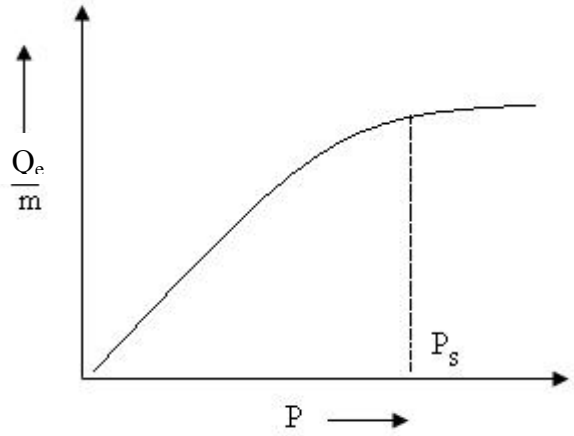

The above graph depicts monolayer adsorption.

This graph can be easily explained using Langmuir adsorption isotherm.

Examples of type I adsorption are adsorption of nitrogen (N_2) or hydrogen (H) on charcoal

Type II Adsorption isotherm

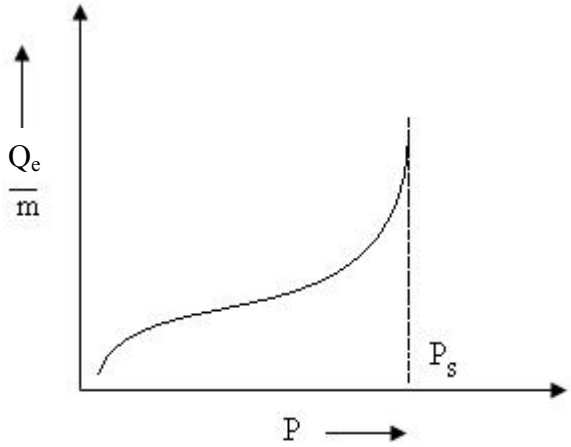

Type II adsorption isotherm shows large deviation from Langmuir model of adsorption.

The intermediate flat region in the isotherm corresponds to monolayer formation.

Examples of type II adsorption are nitrogen (N_2 (g)) adsorbed on iron (Fe) catalyst and nitrogen (N_2 (g)) adsorbed on silica gel.

Type III Adsorption isotherm

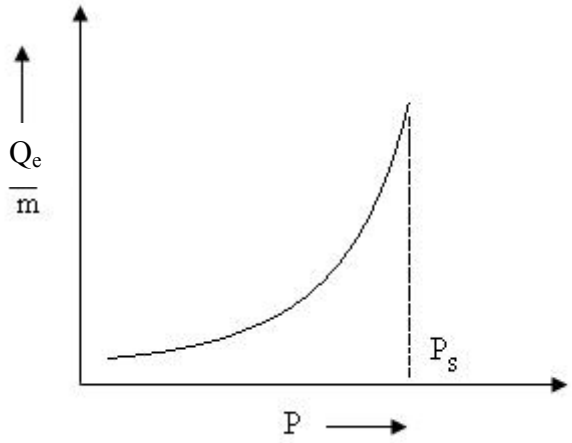

Type III adsorption isotherm also shows large deviation from Langmuir model.

This isotherm explains the formation of multilayer.

There is no flattish portion in the curve which indicates that monolayer formation is missing.

Examples of type III adsorption isotherm are bromine (Br_2) on silica gel or iodine (I_2) on silica gel.

Type IV adsorption isotherm

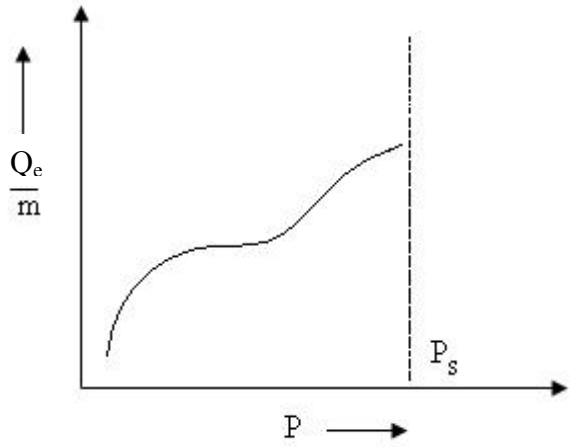

At lower pressure region of graph is quite similar to type II. This explains formation of monolayer followed by multilayer.

The saturation level reaches at a pressure below the saturation vapor pressure. This can be explained on the basis of a possibility of gases getting condensed in the tiny capillary pores of adsorbent at pressure below the saturation pressure (P_S) of the gas.

Examples of type IV adsorption isotherm are of adsorption of benzene on iron oxide (Fe_2O_3) and adsorption of benzene on silica gel.

Type V adsorption isotherm

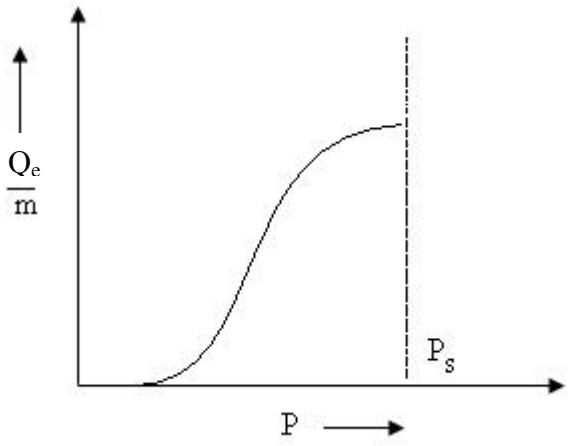

Explanation of type V graph is similar to type IV.

Example of type V adsorption isotherm is adsorption of water (vapors) on charcoal.

Type IV and V shows phenomenon of capillary condensation of gas.

Heat (enthalpy) of adsorption consideration

If the isotherm of adsorption can be fitted with Langmuir model adequately, the heat of adsorption process at monolayer coverage can be investigated from equation (3).

There is another propose that is usually used to explain heat of adsorption. The adsorption data obtained at different temperatures are used to estimate the isosteric heat of the process. Consequently, enthalpy changes associated with adsorption processes can be estimated using the Clausius-Clapeyron equation. The heat of adsorption was calculated by applying the Clausius-Clapeyron equation to the adsorption isotherm as follows (Alberty and Silbey, 1992 and Sirichote, et al., 2002)

$$\frac{dP}{dT} \quad \frac{P \quad H_{vap}}{RT^{2}} \qquad (6)$$

Where P is the equilibrium pressure of gas, T is the absolute temperature, ΔH_{vap} is the heat of vaporization, and R is the gas constant. On rearrangement equation (6) becomes $\frac{dP}{P} \quad \frac{H_{vap}}{RT^{2}} dT$ (7)

The equation (7) can be rewritten as follows

$$d \ln \frac{P}{P_0} \quad \frac{H_{vap}}{RT^{2}} dT \qquad (8)$$

Where P_o is the standard pressure used. Replacement of P by C_eRT and P_0 by C^0RT from ideal gas law where C_e is the equilibrium concentrations (mmol/L) and C^0 is the standard value of the concentration (mmol/L) equation (8) becomes

$$d \ln \frac{C_e}{C^0} \quad \frac{H_{vap}}{RT^{2}} dT \qquad (9)$$

For adsorption in solution the ΔH_{vap} is replaced by ΔH_{ads} which is the heat of adsorption. Integrating on the assumption that the ΔH_{ads} is independent of temperature and concentration and since the term ln C^0 is equal to zero, equation (9) yields

$$d \ln C_e \quad \frac{H_{ads}}{R} \quad T^{\ 2} dT$$

$$\ln C_e \quad \frac{H_{ads}}{RT} \quad c \qquad (10)$$

where C_e is the equilibrium concentrations (mmol L^{-1}), H_{ads} is the isosteric heat of adsorption (kJ mol^{-1}), R is the universal gas constant (8.314 J K^{-1} mol^{-1}) and c is the integration constant. Plot of ln C_e versus 1/T should give a straight line of slope is - (ΔH_{ads} /R). The plots of applied Clausius-Clapeyron equation to adsorption isotherm in equation (10) as ln C_e versus 1/T

1.3 Review of literature

There have been many researches concern in the adsorption of metal ions and dyes on activated carbon surface. This interest is due to the importance of the following processes: surface chemistry, water chemistry, analytical chemistry, chemical engineering and environmental studies. Many researchers have studied adsorption of metal ions and dye on activated carbon such as:

Kadirvelu, et al., (2000) studies the adsorption of three metal ions, Cu^{2+}, Ni^{2+} and Pb^{2+} on activated carbon cloths (ACC). Two adsorbents, CS 1501 (with more than 96% of micropore volume) and RS 1301 (with 32% of mesopore volumn), were studied. Batch experiments were carried out to assess kinetic and equilibrium parameters. They allowed kinetic data, transfer coefficients, and maximum adsorption capacities to be computed. These parameters showed the fast external film transfer of metal ions on fibers because of their low diameter (10 μm). Intraparticular diffusion coefficients are lower than those obtained with a granular activated carbon (GAC), but maximum adsorption capacities agree with literature values for GAC. They showed the dependency of adsorption on metal ion size and ACC porosity, the largest cation Pb^{2+} being more adsorbed by the mesoporous cloth.The pH effect was also studied, and pH adsorption edges were determined. They were short, only 2 pH units,

and located of metal ion concentration, coupled with a regeneration study of saturated ACC by HCl, led them to propose an adsorption mechanism by ion-exchange between metal cations and H^+ ions at the ACC surface. Carboxylic groups seem especially involved in this mechanism, and precipitation between metal ions could happen.

Sirichote, et al., (2002) studied the adsorptions of Fe^{3+} from aqueous solution at room temperature on activated carbons obtaining from bagasse, pericarp of rubber fruit and coconut shell. The activated carbons were prepared by carbonization of these raw materials and followed by activation with $ZnCl_2$. The adsorption behavior of Fe^{3+} on these activated carbons could be interpreted by Langmuir adsorption isotherm as monolayer coverage. The maximum amounts of Fe^{3+} adsorbed per gram of these activated carbons were 0.66, 0.41, and 0.18 mmol g^{-1}, respectively. Study of the temperature dependence on these adsorptions has revealed them to be exothermic processes with the heats of adsorption of about -8.9, -9.7, and -5.7 kJ mol^{-1} for bagasse, pericarp of rubber fruit and coconut shell, respectively.

Strelko, et al., (2002) oxidized a commercial activated carbon Chemviron F 400 by using nitric acid in order to introduce a variety of acidic surface functional groups. Both unoxidized and oxidized carbon samples were characterized using nitrogen porosimetry (nitrogen adsorption isotherm), elemental analysis, pH titration, Boehm's titration, and electrophoretic mobility measurements. Results showed that oxidation treatment reduced surface area and pore volume. However, the carbon surface acquired an acidic character with carboxylic groups being the dominant surface functional groups. The modified sample displayed cation-exchange properties over a wide range of pH values and exhibits polyfunctional nature. Both carbon samples were challenged for the removal of transition metals such as Cu^{2+}, Ni^{2+}, Co^{2+}, Zn^{2+} and Mn^{2+}.The affinity series $Mn^{2+} < Co^{2+} < Ni^{2+} < Cu^{2+} < Zn^{2+}$ have been found to coincide with the general stability sequence of metal complexes (the Irving-Williams series).

Savova, et al., (2003) studied on the adsorption manganese ions from aqueous solution on carbon obtained from a mixture of biomass products (apricot

stones). They indicated the importance of acidic surface oxides for manganese ion adsorption that was predominantly site specific. The results showed that oxygen remaining from the raw material participates in the formation of surface oxides and indicated the possibility of controlling the content of acidic surface sites of the carbon surface by appropriate selection of the precursor composition and surface properties modification. The surface functionalities of oxidized carbon from a mixture of biomass products resembled the behavior of an ion-exchange resin. Oxidized carbon obtained from a 50:50 mixture of tar from steam pyrolysis of apricot stones and furfural contained a balance of surface area and high surface concentration of functional groups was favorable for adsorption of positively charged manganese ions.

Bhatnagar, et al., (2004) reported four adsorbents have been prepared from industrial wastes obtained from the steel and fertilizer industries and investigated for their utility to remove cationic dyes. Studies have shown that the adsorbents prepared from blast furnace sludge, dust, and slag have poor porosity and low surface area, resulting in very low efficiency for the adsorption of dyes. On the other hand, carbonaceous adsorbent prepared from carbon slurry waste obtained from the fertilizer industry was found to show good porosity and appreciable surface area and consequently adsorbs dyes to an appreciable extent. The adsorption of two cationic dyes, viz., Rhodamine B and Bismark Brown R on carbonaceous adsorbent conforms to Langmuir equation, is a first-order process and pore diffusion controlled. As the adsorption of dyes investigated was appreciable on carbonaceous adsorbent, its efficiency was evaluated by comparing with those obtained on a standard activated charcoal sample. It was found that prepared carbonaceous adsorbent exhibits dye removal efficiency that is about 80–90% of that observed with standard activated charcoal samples. Thus, it can be fruitfully used for the removal of dyes and is a suiTable alternative to standard activated charcoal in view of its cheaper cost.

Kadirvelu, et al., (2005) studied the activated carbon which prepared by using industrial solid waste called sago waste and physico-chemical properties of carbon were carried out to explore adsorption process. The effectiveness of carbon prepared from sago waste in adsorbing Rhodamine B from aqueous solution has been

studied as a function of agitation time, adsorbent dosage, initial dye concentration, pH and desorption. Adsorption equilibrium studies were carried out in order to optimize the experimental conditions. The adsorption of Rhodamine B onto carbon followed second order kinetic model. Adsorption data were modeled using both Langmuir and Freundlich classical adsorption isotherms. The adsorption capacity Q_0 was 16.12 mg g^{-1} at initial pH 5.7 for the particle size 125–250 μm. The equilibrium time was found to be 150 min for 10, 20 mg L^{-1} and 210 min for 30, 40 mg L^{-1} dye concentrations, respectively. A maximum removal of 91% was obtained at natural pH 5.7 for an adsorbent dose of 100 mg/50 mL of 10 mg L^{-1} dye concentration and 100% removal was obtained when the pH was increased to 7 for an adsorbent dose of 275 mg/50 ml of 20 mg L^{-1} dye concentration. Desorption studies were carried out in water medium by varying the pH from 2 to 10. Desorption studies were performed with diluted HCl and show that ion exchange is predominant dye adsorption mechanism. This adsorbent was found to be both effective and economically viable.

Arivoli, et al., (2007) studied a carbonaceous adsorbent which was prepared from Phoenix Sylvestric (PSC) by acid treatment and was tested for its efficiency in removing Rhodamine B (RDB). The parameters studied include agitation time, initial dye concentration, carbon dose, pH and temperature. The adsorption followed first order reaction equation and the rate is mainly controlled by intra-particle diffusion. Freundlich and Langmuir isotherm models were applied to the equilibrium data. The adsorption capacity (Q_m) obtained from the Langmuir isotherm plots were 51.546, 47.236, 44.072 and 41.841 mg/g, respectively at an initial pH of 7.0 at 30, 40, 50 and 60 $^{\circ}$C. The temperature variation study showed that the Rhodamine B adsorption is endothermic and spontaneous with increased randomness at the solid solution interface. Significant effect on adsorption was observed on varying the pH of the Rhodamine B solutions. Almost 90% removal of Rhodamine B was observed at 60 $^{\circ}$C. The Langmuir and Freundlich isotherms obtained, positive H^0 value, pH dependent results and desorption of dye in mineral acid suggest that the adsorption of Rhodamine B on PSC involves physisorption mechanism.

Sirichote, et al., (2008) reported activated carbons prepared from bagasse, oil palm shell and pericarp of rubber fruit were used to study the adsorption of phenol

from aqueous solution. The obtained activated carbons were characterized for iodine number, BET surface area, surface functional groups, and point of zero charge (pH_{pzc}). The values of BET surface area of bagasse, pericarp of rubber fruit and oil plam shell were 1076, 877, 770 m^2 g^{-1}, respectively. Adsorption of phenol in aqueous solution at pH 2 and pH 12 were determined by UV-Visible spectrophotometer at maximum wavelength 233 nm and 287 nm, respectively and 30°C. The adsorption data were fitted to Freundlich isotherm. The adsorption capacity of phenol of the different types of activated carbon was approximately the same. The adsorption capacity of phenol at pH 2 is greater than at pH 12 because of pH 2 the surfaces of activated carbons are protonated and have acidic surfaces with positive charges. Phenol behaves as a weak base that interacts with the acidic surface of activated carbons by dispersion electron donor-acceptor interaction.

Arivoli, et al., (2009) studied a carbonaceous adsorbent which was prepared from banana bark by acid treatment and was tested for its efficiency in removing Rhodamine B (RDB). The parameters studied include agitation time, initial dye concentration, carbon dose, pH and temperature. The adsorption followed first order kinetics and the rate is mainly controlled by intra-particle diffusion. Freundlich and Langmuir isotherm models were applied to the equilibrium data. The maximum amounts of dye (Q_m) adsorbed per gram of these activated carbons obtained from the Langmuir isotherm plots were 40.161, 35.700, 38.462 and 37.979 mg g^{-1} respectively at an initial pH of 7.0 at 30, 40, 50 and 60 °C. The temperature variation study showed that the RDB adsorption is endothermic. Almost 85% removal of RDB was observed at 60 °C.

1.4 Objectives

1.4.1 To characterize some physical and chemical properties of the commercial activated carbon and activated carbon obtained from pericarp of rubber fruit.

1.4.2 To study the dependence of variable parameters on the adsorption of Rhodamine B on commercial activated carbon and activated carbon obtained from pericarp of rubber fruit.

1.4.3 To study the adsorption isotherm of Rhodamine B on commercial activated carbon and activated carbon obtained from pericarp of rubber fruit.

CHAPTER 2

METHOD OF STUDY

2.1 Chemicals and materials

1. Commercial activated carbon (CAC); Sigma – Aldrich, USA
2. Rhodamine B; Fluka, UK
3. Sodium chloride, NaCl; A.R., Assay 98%, Merck, Germany
4. Sodium hydroxide, NaOH; A.R., Assay 99%, Lab Scan Ireland
5. Hydrochloric acid, HCl; A.R., 37%, Merck, Germany
6. Potassium bromide, KBr; IR grade, Merck, Germany

2.2 Equipments and Instruments

2.2.1 Department of Chemistry, PSU

1. Centrifuge; MSE, HOMOGENISER, UK
2. Analytical balance; AB 204 – S, METTLER TOLEDO, Switzerland
3. pH meter; WTW Inolab pH level 1, Germany
4. Oven; UFE 500, Memmert, Germany
5. Hotplate and stirrer; Heidolph MR 3001, Jenway, UK
6. Thermostat shaker water bath; Memmert, Germany
7. Test sieve and lid receiver; 100 – 140, 140 - 170 and 170 - 200 mesh U.S., Endecotts
8. UV-Visible spectrophotometer; SHIMADZU UV-160A, Japan
9. Fourier-transform infrared spectrophotometer and diffuse reflectance accessory, FT-IR and KBr techniques; Spectrum GX, Perkin Elmer, U.S.

2.2.2 Scientific Equipment Center, PSU

Scanning electron microscope (SEM; JSM-5800 LV, JEOL: Attached with energy dispersive X-ray spectrometer (EDS; Oxford ISIS 300)

2.2.3 Department of Chemical Engineering, PSU

Surface area and pore size analyzer; SA 3100, Coulter

2.3 Methods

2.3.1 Preparation of activated carbon obtained from pericarp of rubber fruit (PrAC)

The production processes of activated carbon from pericarp of rubber fruit were carbonization and chemical activation with $ZnCl_2$. Pericarp of rubber fruit was dried in the sun and cut into small pieces approximately 1 inch and placed into stainless steel box with cover.

The carbonization was then conducted in a in a muffle furnace at 400 ^{o}C for 1 h. After carbonization the residual char was grounded in a laboratory jar mill to pass between 200-270 mesh sieves. Then, the chemical activation was performed by mixing the grounded char with concentrated solution of $ZnCl_2$ at ratio 1:2. The sample was activated at 600 ^{o}C for 3 h in the muffle furnace (Sirichote et al., 2002). The obtained activated carbon was washed with 1% HCl. In the next step, it was soaked in hot water for five minutes and subsequently the water was drained off through a Buchner funnel. This step was repeated two more times to obtain a neutral pH value. Finally, it was dried in the oven at 110 ^{o}C for 24 h. The obtained activated carbon was kept in a dessicator (Sirichote et al., 2008). (The PrAC was prepared by bachelor's degree student in chemistry project at Department of Chemistry, PSU.)

2.3.2 Characterization of activated carbon surfaces

2.3.2.1 Surface area and pore size analysis

Nitrogen adsorption isotherms at 77 K carried out with Coulter model SA 3100 apparatus were used to determine specific surface areas (BET surface areas) and micropore volumes of activated carbons by using Brunauer-Emmett-Teller (BET) and t-plot equations, respectively. The pore size distribution was calculated by using the Barrett-Joyner-Halenda (BJH) model (program for calculation these parameters is already in this apparatus) (Barrett, et al., 1951). Prior to the nitrogen adsorption experiments, for maintaining the integrity of the chemical surface properties, all samples were degassed for 1 hour at 120°C. (The measurement was conducted at Department of Chemical Engineering, PSU.)

2.3.2.2 Scanning electron microscopy (SEM)

A scanning electron microscope JSM-5800 LV located at Scientific Equipment Center, PSU was used to analyze the porosity of activated carbon samples.

2.3.2.3 Fourier-transform infrared spectrophotometry (FT-IR)

Activated carbon samples were studied spectroscopically with Fourier-transform infrared spectrophotometry, FT-IR. The transmission IR spectra of the carbon samples were obtained using KBr technique. The KBr disks were prepared by activated carbon-KBr mixtures in a ratio about 1:300 which were finely ground by pestle in an agate mortar and then dried at 120°C in oven and finally pressed in a hydraulic press (KBr pellet presser). Before the spectrum of a sample was recorded, the background line was obtained arbitrarily and subtracted. The spectra were recorded from 4000 to 400 cm^{-1} at a scan rate of 0.2 cm s^{-1}, and for the best resolution, the numbers of interferogram at a nominal resolution of 4 cm^{-1} was scanned more than 10 times.

2.3.2.4 Point of zero charge measurements (pH_{pzc})

By using the pH drift method (Jia, et al., 1998), the pH at the potential zero charge (pH_{pzc}) of various activated carbons was measured. The pH of a solution of 0.1 M NaCl was adjusted between 2 - 12 by using 0.01 mol L^{-1} HCl or NaOH. Activated carbon sample (0.2000 and 0.6000 g) was added into 100 mL of NaCl solution in 250 mL flask. The flasks were sealed, to eliminate any contact with air and then left at ambient temperature. The final pH was recorded after the pH had stabilized (typically after 24 h). The point at which initial pH and final pH were the same value was determined by using the graph of final pH versus initial pH. This was taken as the pH_{pzc} of the activated carbon.

2.3.3 Adsorption studies

2.3.3.1 Adsorbate (dye solution)

The dye used in this study is Rhodamine B. Its molecular weight is 479.02 g mol^{-1}. Adsorbate stock solution, 1000 mg L^{-1} was prepared by dissolving in distilled water. Then the stock solution was diluted with distilled water to obtain series of standard solutions with concentrations ranging from 150-500 mg L^{-1}

2.3.3.2 Effect of variable parameters

Weight of activated carbon

The various doses of the activated carbon were mixed with the dye solutions and the mixtures were agitated in a mechanical thermostat shaker at 30°C. The adsorption capacities for different doses were determined at definite time intervals by keeping initial concentration of dye, contact time, and pH constant.

Initial concentration of dye

Experiments were conducted with different initial concentrations of dyes ranging from 150 - 500 mg L^{-1}. Weight of activated carbon, contact time, and pH were kept constant.

Contact time

The effect of contact time on the adsorption of dye by the adsorbent in a single cycle was determined by keeping particle size of activated carbon, pH and initial concentration of dye constant.

Temperature

The adsorption experiments were performed at 30, 40, 50 and 60 °C in a thermostat - attached water bath shaker.

pH

The pH of Rhodamine B solution of 300 mg L^{-1} was adjusted between 2 - 13 by using 0.01 mol L^{-1} HCl or 0.01 mol L^{-1} NaOH. Activated carbon sample (0.02 g and 0.09 g for commercial activated carbon (CAC) and pericarp of rubber fruit activated carbon (PrAC), respectively) was added to 50 mL of dye solution. The contents were then shaken at 30 °C in the thermostat shaker water bath. After the equilibrium was obtained (more than 6, 24 h for CAC, PrAC), about 2 mL was transferred to test tube and centrifuge. The supernatant was decanted and analyzed for the concentration of Rhodamine B.

2.3.3.3 Adsorption isotherm studies of Rhodamine B on activated carbons

By adding 0.02 g of CAC and 0.09 g of PrAC to 50 mL of Rhodamine B solution, adsorption equilibrium studies of Rhodamine B on CAC and PrAC were carried out in a batch process at 30, 40, 50 and 60 °C. The concentrations of solutions at pH 4 were varied in the range of 150 – 450 mg L^{-1}. The contents were centrifuged after gentle shaking for 6 h and 24 h for CAC and PrAC, respectively, in a thermostat shaker water bath. Rhodamine B concentrations before and after adsorption were then determined by UV-Vis spectrophotometer at a wavelength 554 nm. The amounts of Rhodamine B adsorbed were calculated based on the difference between the Rhodamine B concentration in aqueous solution before and after adsorption. The amount adsorbed was calculated from the equation.

$$Q_e \quad \frac{V(C_0 \quad C_e)}{W} \qquad (11)$$

where Q_e is the amounts of dye adsorbed onto activated carbon (mg g^{-1}), V is the volume of the solution (L), C_0 is the initial liquid- phase concentration of dye (mg L^{-1}), C_e is the equilibrium liquid- phase concentration of dye (mg L^{-1}), and W is the weight of the adsorbent (g). The amount of dye adsorbed on to activated carbon was calculated based on the previously determined calibration curve.

CHAPTER 3

RESULTS AND DISCUSSION

3.1 Characterization of activated carbons surfaces

3.1.1 Scanning electron microscopy (SEM)

In Figure 2, the scanning electron micrographs of the external structures of two activated carbon, CAC 200 – 270 mesh and PrAC 200 – 270 mesh, are shown. From micrographs, it can be seen that CAC 200 – 270 and PrAC 200 – 270 are full of holes with diameters ranging from around 7.5 – 10.5 μm and 4 - 20 μm, respectively. These holes are defined as macropore of the activated carbon (>50 nm). Both the micropore and mesopore are not resolved by scanning electron microscopy even at higher magnification because of the limit of detection of instrument.

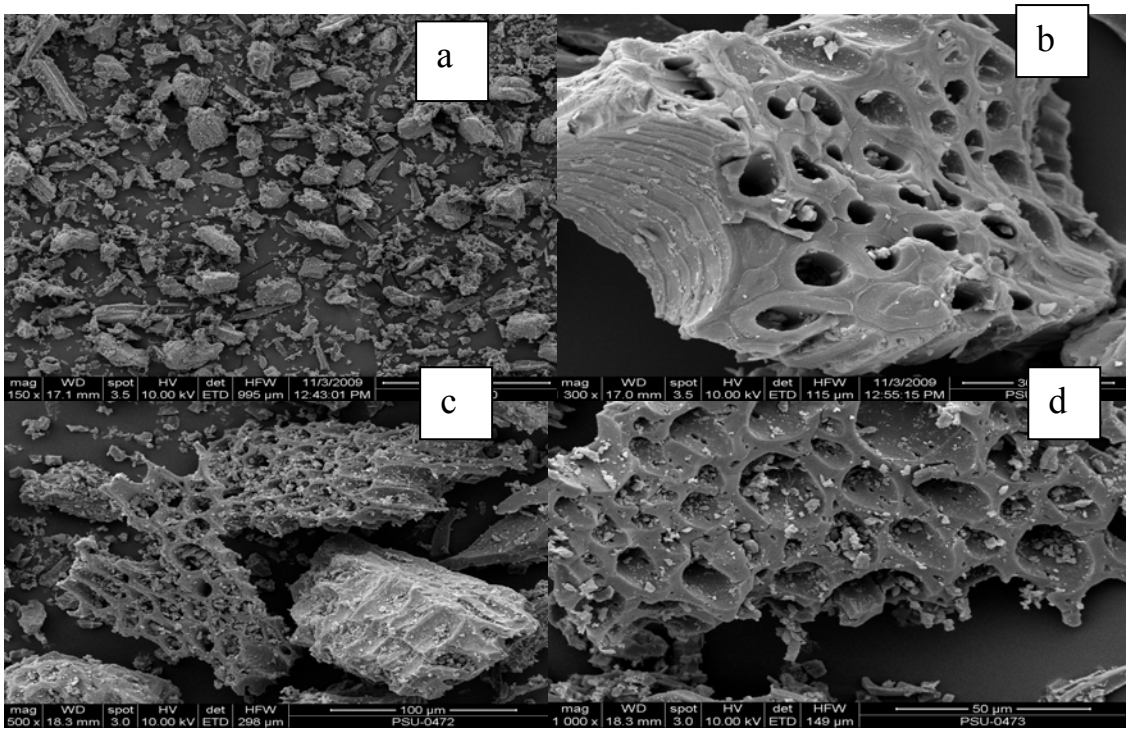

Figure 2 SEM micrographs of (a) CAC-200-270 (150), (b) CAC- 200-270 (1300), (c) PrAC- 200-270 (500), and (d) PrAC- 200-270 (1000) activated carbons.

3.1.2 Surface area and pore size analysis (physical or porous texture characterization)

By the construction of N_2 adsorption isotherms, an understanding of the surface area and porosity of an adsorbent can be achieved. The adsorption volume of adsorbent was measured over a wide range of relative pressures at constant temperature (77 K). Nitrogen adsorption isotherms measured for CAC and PrAC activated carbon were shown in Figure 3. It is evident that all isotherms can be classified into two types.

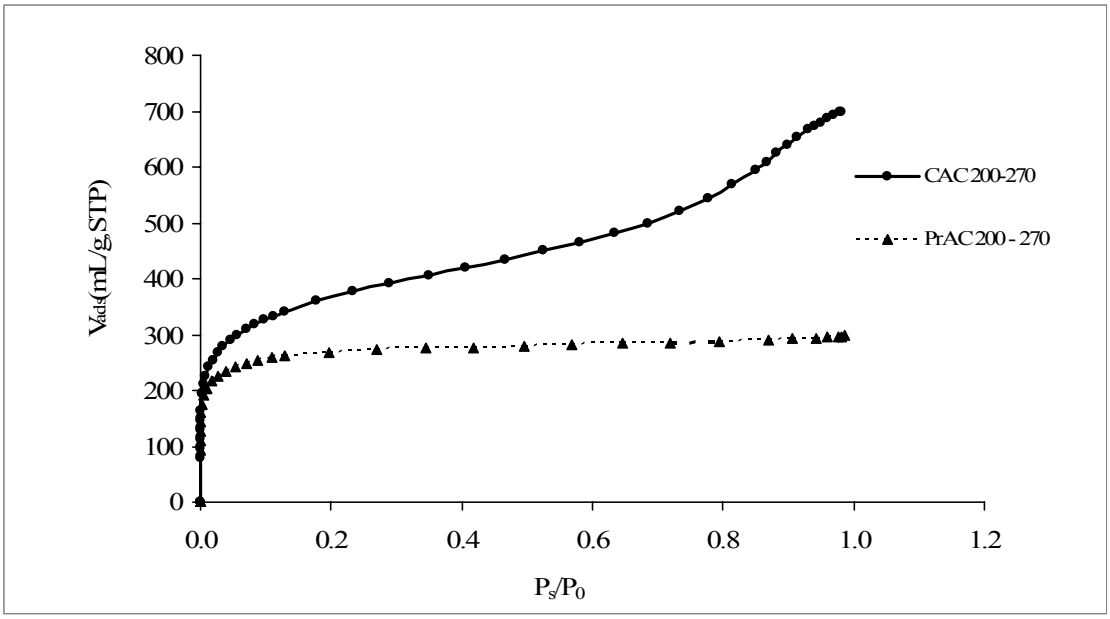

Figure 3 Adsorption isotherms of N_2 at 77 K for the CAC and PrAC (P_s/P_0 is relative pressure).

In the case of PrAC, the sample is approximately type I according to IUPAC classification (Hu and Vansant, 1995) since most of the adsorbed volume is contained in the micropores. Its isotherms shows the steep rise of the initial part of the isotherms where micropores is filled by nitrogen molecule completely at ~0.2 P/P_0. After 0.2 P/P_0, the isotherms become plateau. It is now widely accepted that the initial part of the type I isotherm represented micropore filling and that the slope of the plateau at high relative pressure is due to monolayer adsorption on the nonmicroporous structures, such as in mesopores, in macropores, and on the external surface. It can be assumed that its material have significant micropores if nitrogen adsorption isotherm

of any porous material can be fitted with type I isotherm. Thereby, PrAC have the contents largely of micropore. On the other hand, isotherms of PrAC belong to a mixed type in the IUPAC classification (Juang, et al., 2002). In the initial parts it is type I, with an important uptake at low relative pressures. It is type II at intermediates and high relative pressures. The steep rise of the initial part of the isotherms evidences the presence of micropores. However, the present samples do not reach a clear plateau unlike other activated carbons. This indicated that CAC and PrAC are mainly micro- and mesoporous in character with a minor presence of wider pores where capillary condensation occurred.

Table 1 BET and micropore surface areas of CAC and PrAC.

Samples	**BET surface areas (m^2 g^{-1})**	**Micropore surface areas (m^2 g^{-1})**	**Micropore fractions (%)**	**Micropore volumes (mL g^{-1})**
CAC 200-270	1,316.90	492.40	37.39	0.20
PrAC 200-270	920.69	698.26	75.84	0.32

From Table 1, futher understanding in porous characters of all carbons can be observed. The results show that all of the samples possess a well-developed porous structure. CAC and PrAC exhibit different BET surface areas. The difference among BET surface area of both samples is about 30%. Hence, BET surface areas may affect the adsorption efficiency in this study.

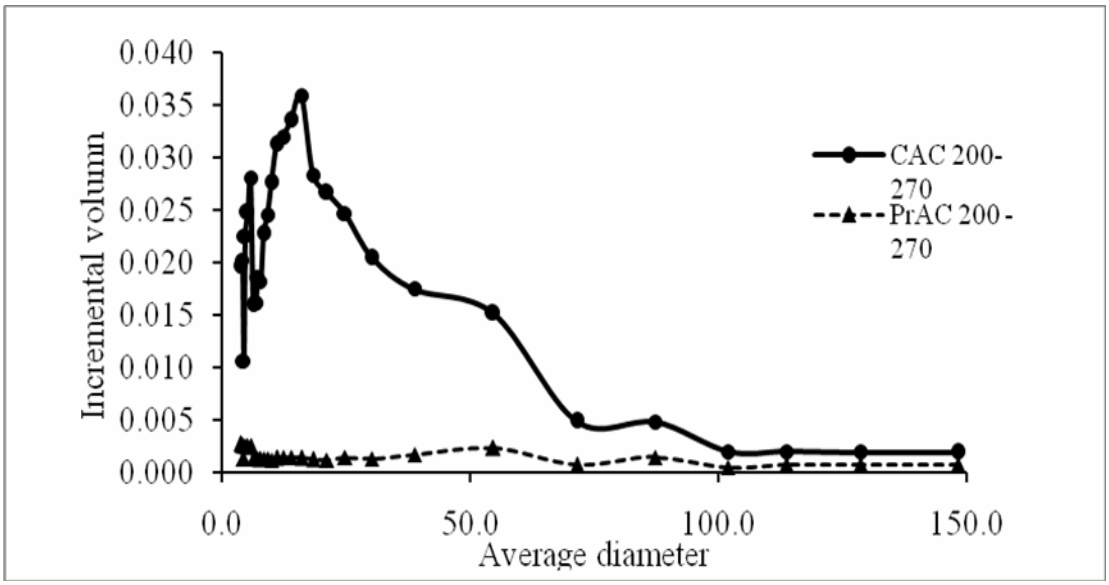

Figure 4 BJH pore size distribution of CAC and PrAC.

Generally, the pores of activated carbon are classified into three groups, micropore (< 2 nm), mesopore (2-50 nm) and macropore (> 50 nm). In this study, however, pore size distribution in the micropore region cannot be measured due to the limitation of instrument. There are many methods for determinations of pore size distribution in the micropore region. Methods based on the potential theory of Dubinin, t-plot method, α plot or MP methods (Strelko and Malik, 2002) are widely used for micropore evalution. This research has used t-plot method for determining micropore surface area, micropore fraction and micropore volume but this method cannot be used for determination of the distribution of micropore. Pore size distribution above 2 nm, however, can be assessed accurately using the method of Barrett, Joyner and Halenda (BJH) model (Barrett, et al., 1951).

It can be seen from Table 1 that PrAC possesses more micropore surface areas and percentages of micropore fraction ((micropore surface area/ BET surface area) ×100) around 75% which is more than the CAC. Noticeably, CAC has more BET surface areas than PrAC but CAC shows less micropore fraction. From Figure 4, CAC remarkably has more incremental pore volume of mesopore and macropore than PrAC. Therefore, the physical characteristics of raw materials seem to be important factor for porous nature of activated carbon.

Figure 4 shows the meso- and macropore nature (>2 nm) of all activated carbon. PrAC do not have significant mesopores and macropores. In contrast, CAC possesses a significant amount of mesopore with a maximum at 6 nm and 16 nm. PrAC also shows the evidence of the presence of mesopores and macropores. The presence of mesopores and macropores of CAC may affect to reduction of micropores while its BET surface area is highly remained.

3.1.3 Fourier-transform infrared spectrophotometry (FT-IR)

The assignment of a specific wave number to a given functional group is not possible although numerous FT-IR spectroscopic studies have been conducted on various forms of carbon because the characteristic bands of various functional groups overlap and shift, depending on their molecular structures and environments (Fuente, et al., 2003). Nonetheless, a consensus in the assignment of band frequencies to different functional groups is possible to a certain extent.

In Figure 5, the spectra of two activated carbons are shown. The strong band appears at about 3,400 cm^{-1} is mainly assigned to O-H stretching vibrations. The band observed at about 2,900 cm^{-1} which is ascribed to symmetric and asymmetric C-H stretching vibrations in aliphatic CH, CH_2 and CH_3 groups are detected. The bands at about 1,600 cm^{-1} is C=C stretching vibration in aromatic rings. Many bands belonging to hydrogen, oxygen, and nitrogen functional groups are observed in the range 1,400 - 400 cm^{-1} which is difficult to assign each simple motion of specific functional groups except the strong band at about 1,015 cm^{-1} can be attributed to C-O stretching vibrations. The both activated carbon samples show very similar spectra (Buczek, et al., 1999).

As mentioned above, all activated carbon samples have similar spectra. It does not mean chemical nature of activated carbons will not be different. Unfortunately, FT-IR can be used only to characterize functional groups on the carbon surfaces qualitatively. Quantitative analysis by using this method is difficult to distinguish the nature of carbons. It is necessary to employ other methods for clear chemical characterizations.

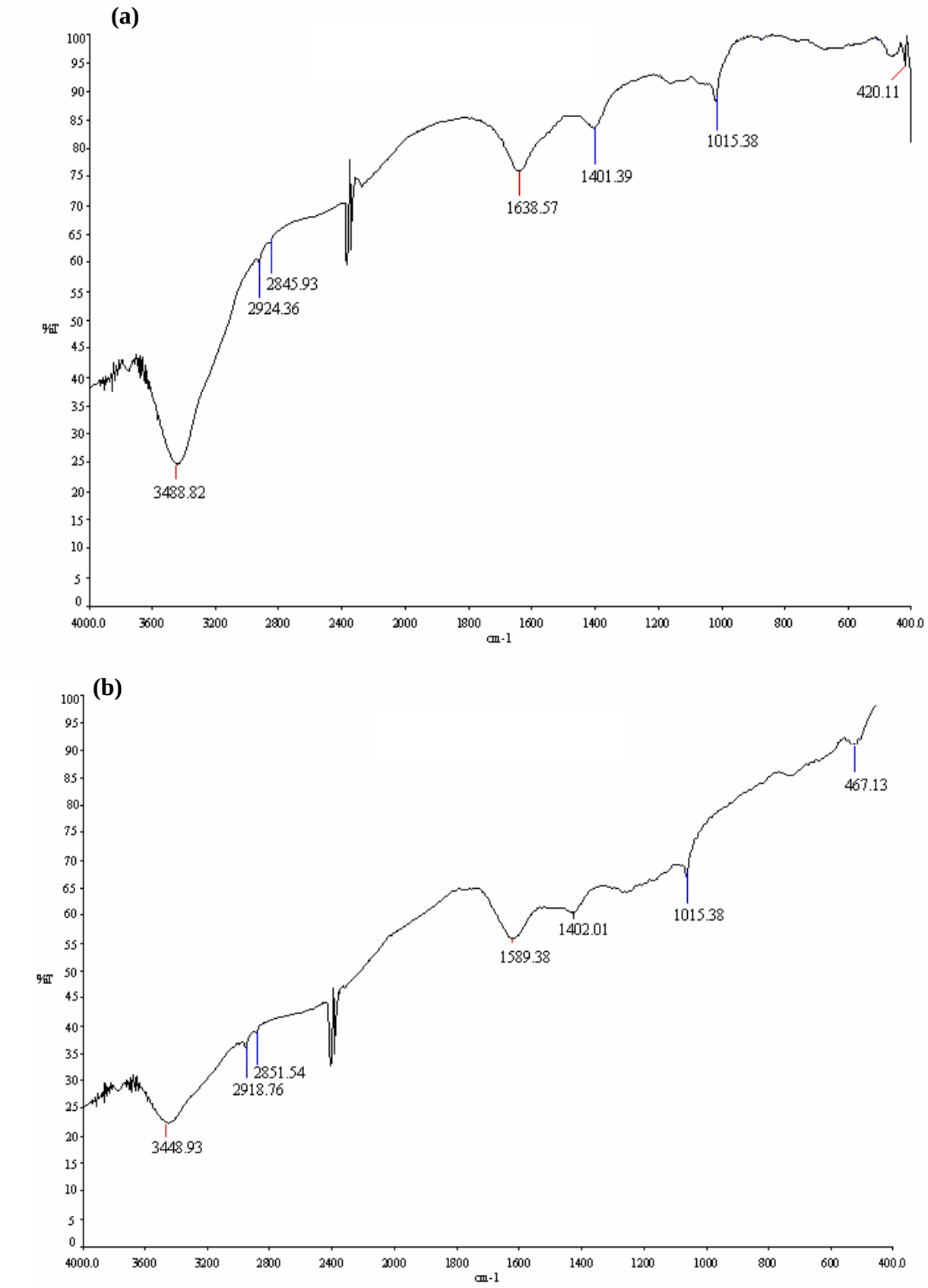

Figure 5 FT-IR Spectra of (a) CAC, and (b) PrAC.

3.1.4 Point of zero charge measurements (pH_{pzc})

In Figure 6, the graphs of final pH versus initial pH obtained by using pH drift method (Jia, et al., 2002) for all activated carbon samples. The result shows that pH_{pzc} of CAC is 3.5 indicating the CAC has acidic surface nature while pH_{pzc} of PrAC is 6.5 indicating the surface nature of PrAC is weakly acidic. The graph of final pH (pH_f) versus initial pH (pH_0) is used to determine the points at which initial pH and final pH values were equal. This point is taked as the pH_{pzc} of the activated carbon.

(a)

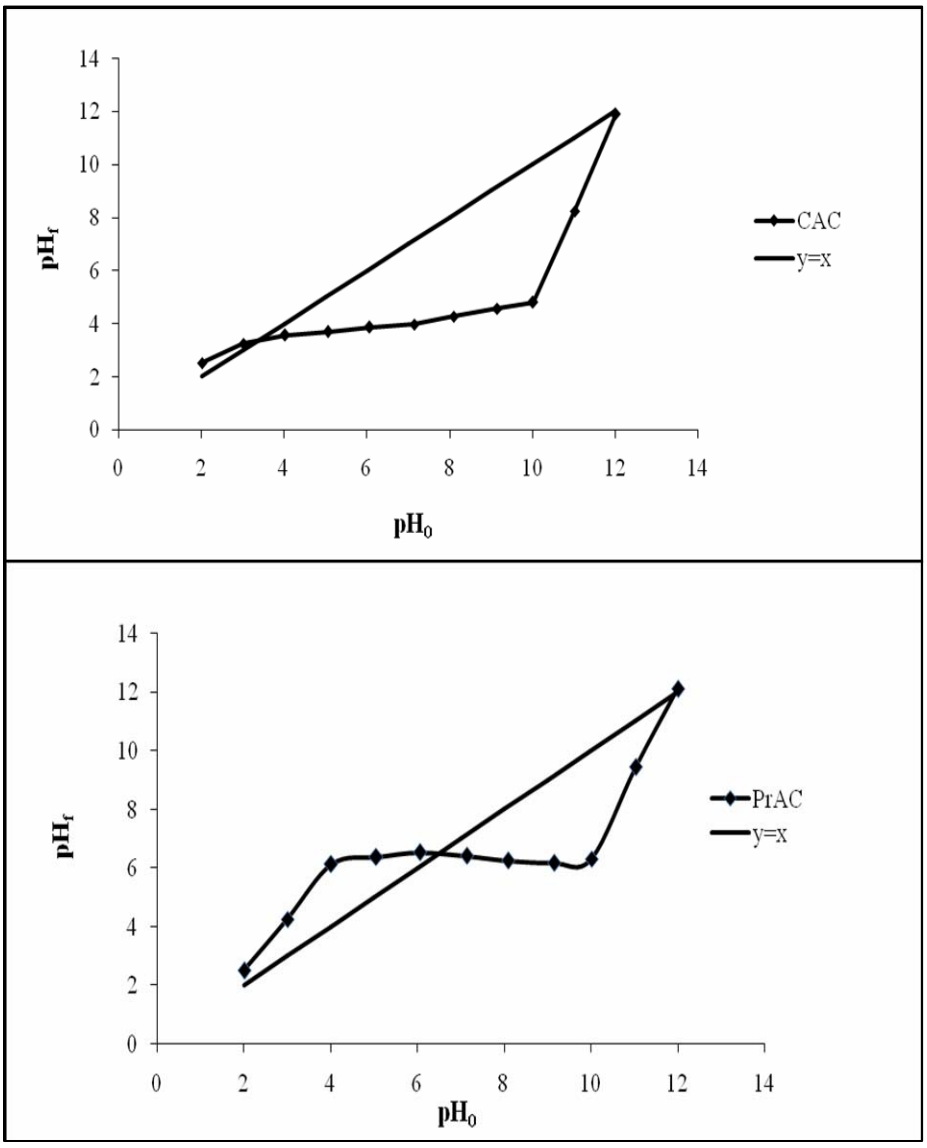

(b)

Figure 6 Graphs of final pH versus initial pH for determination the point of zero charge (pH_{pzc}) of CAC – 200 – 270 (a) and PrAC – 200 – 270 (b).

The amphoteric character of surface oxides S-CO_2 where S represents the activated carbon surface can be explained as follows (Kadirtvalu, et al., 2000).

For pH < pH_{pzc}, the dominant reaction is:

$$S\quad CO_2\quad 2H_2O\qquad S\quad C(OH\ )_2\quad 2OH$$

The release of hydroxyl ions induces an increase of pH and a protonated surface of activated carbon.

For pH> pH_{pzc} , the following reaction takes place:

$$S\quad CO_2\quad 2H_2O\qquad S\quad C(O\ )_2\quad 2H_3O$$

The activated carbon surface is deprotonated and the release of protons induces a decrease in pH.

The pH and acid-base values of the activated carbon give a good indication of the surface oxygen complexes and the electrical surface changes undergone by them. These surface changes arise from the interaction between the carbon surface and the aqueous solution. The complexes on the carbon surfaces are generally classified as acidic, basic, and neutral groups.

3.2 Adsorption studies

3.2.1 Spectroscopy of Rhodamine B

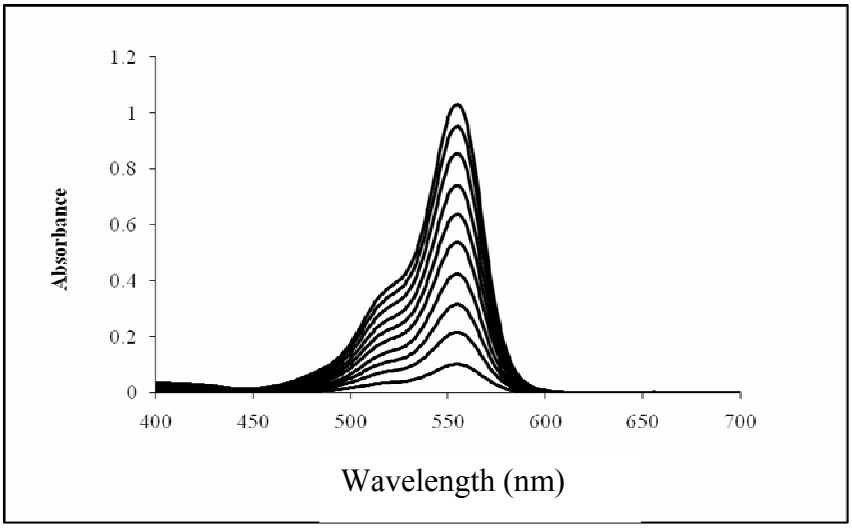

Figure 7 Spectra of 0.5 – 5 mg L^{-1} Rhodamine B.

Figure 7 shows the concentration of Rhodamine B in aqueous solution as determined by UV-Vis spectrophotometer at maximum wavelength of 554 nm.

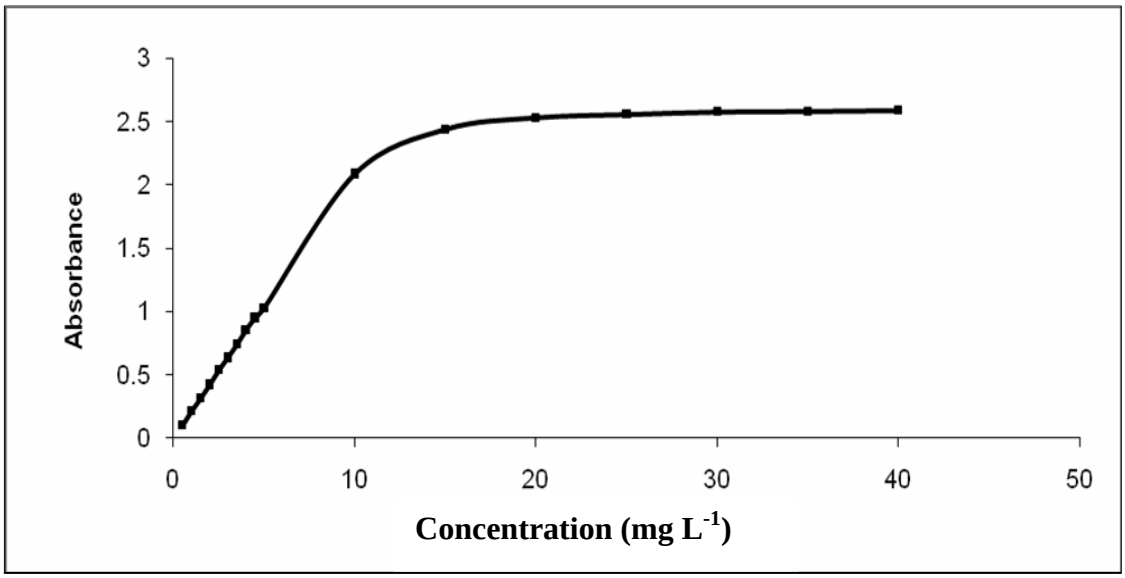

Figure 8 Relation of absorbance with 0.5 – 40 mg L^{-1} Rhodamine B (at $_{max}$ = 554 nm, room temperature).

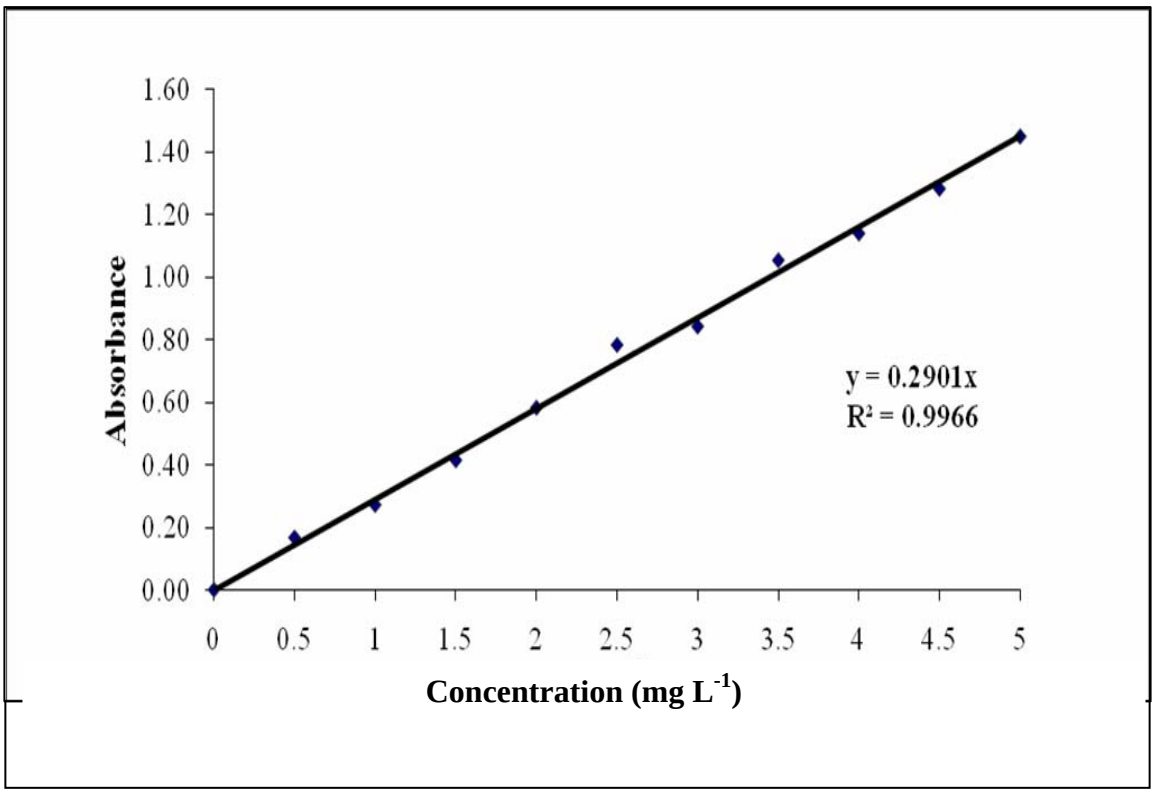

Figure 9 Standard curve of Rhodamine B solution (0 – 5 mg L^{-1}, at $_{max}$ = 554 nm)

3.2.2 Adsorbate dye solution

Concentration range of Rhodamine B was used in this study is 150 to 500 mg L^{-1}, which is completely dissolved in water.

The structure of Rhodamine B in aqueous solution is shown below.

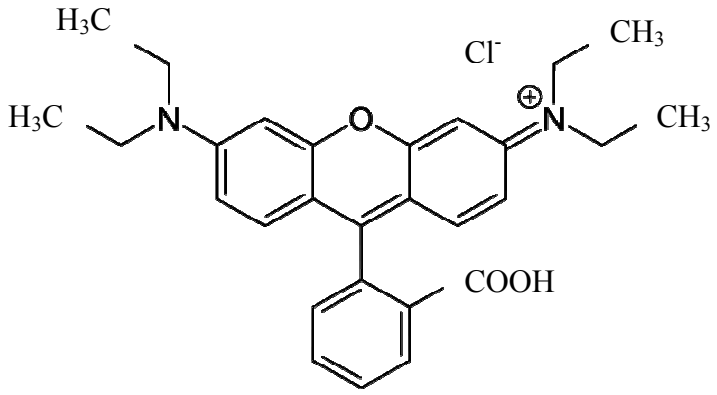

3.2.3 Effect of various parameters

3.2.3.1 Weight of activated carbon

The adsorption of Rhodamine B onto the 200 – 270 mesh CAC and PrAC (Bhatnagar, 2005) were studied by varying the weights of activated carbon in the ranges of 0.010 - 0.035 g/50 mL and 0.05 – 0.10 g/50 mL for 300 mg L^{-1} of dye concentration, respectively, at pH 4 which is pH nature of dye solution. The percentage of adsorption increased with increasing weight of both activated carbons as shown in Figure 10 and Figure 11, respectively. Effect of weight of activated carbon was attributed to the increase of surface area and availability of more adsorption sites (Namasivayam, et al., 1996). In this study, the appropriate weight of CAC and PrAC is 0.02 and 0.09, respectively for adsorption of Rhodamine B.

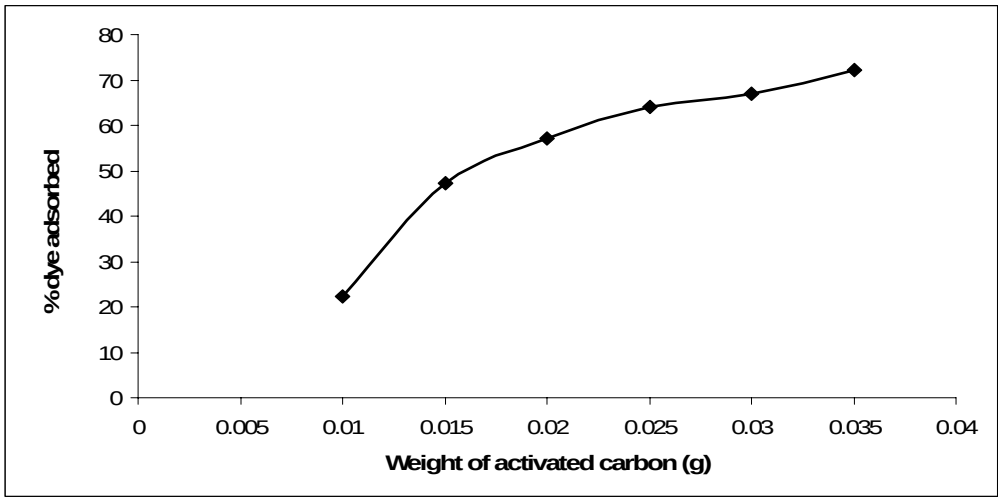

Figure 10 Effect of weight of CAC (200 – 270 mesh), 0.01 – 0.035 g/50 mL at 30°C, pH = 4 and dye concentration 300 mg L^{-1}.

.

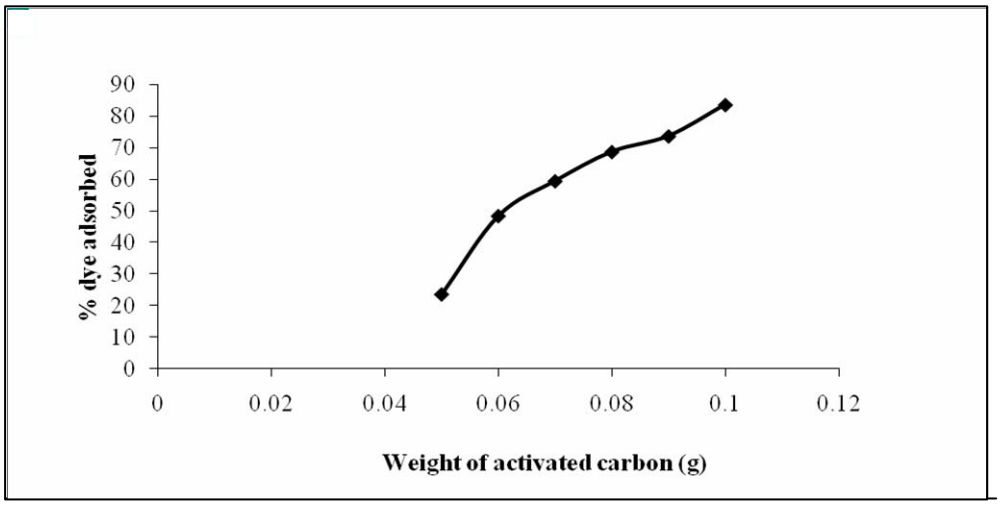

Figure 11 Effect of weight of PrAC (200 – 270 mesh), 0.05 – 0.1 g/50 mL at 30°C, pH = 4 and dye concentration 300 mg L^{-1}.

.

3.2.3.2 Effect of contact time and initial dye concentration

The adsorption of Rhodamine B onto the CAC and PrAC were studied in order to assess the time required for equilibrium to be achieved. In most adsorption isotherm studies, the results showed that equilibrium was achieved within around 6 h. and 24 h. for CAC and PrAC as shown in Figure 12 and Figure 13, respectively. However, the solutions were left longer than equilibrium time to ensure complete equilibration.

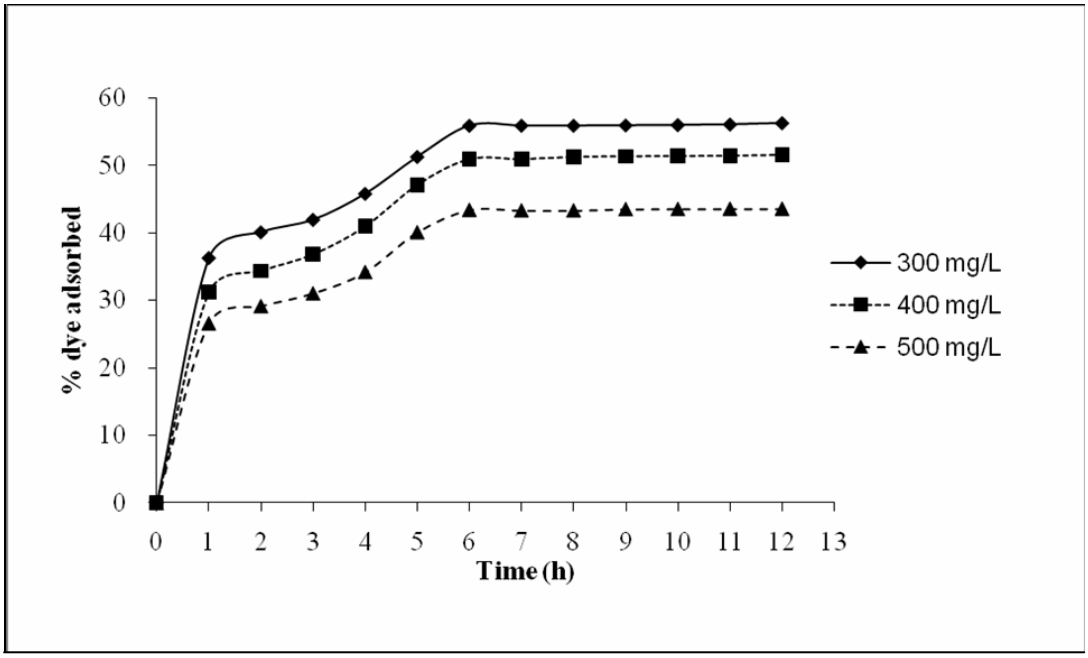

Figure 12 Equilibrium time of 300, 400 and 500 mg L^{-1} Rhodamine B on CAC at 30°C and pH = 4.

.

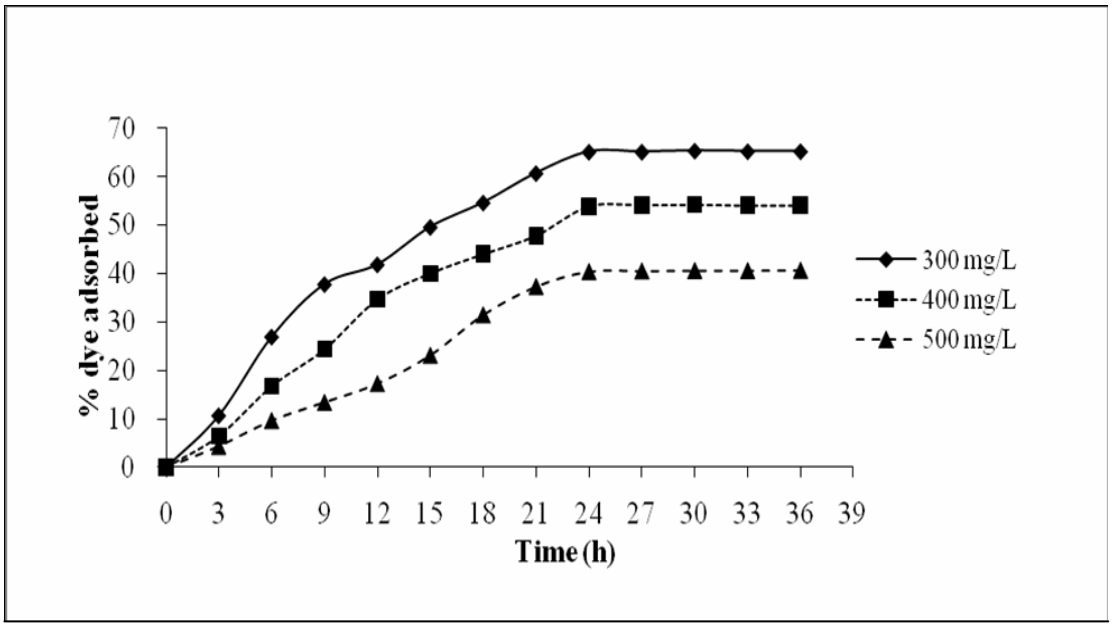

Figure 13 Equilibrium time of 300, 400 and 500 mg L^{-1} Rhodamine B on PrAC at 30°C and pH = 4.

3.2.3.3 Effect of pH

The pH of Rhodamine B solution decreased with increasing concentration of Rhodamine B as shown in Table 2 due to the increasing in amount of proton which release from Rhodamine B.

Table 2 The pH of aqueous solution of Rhodamine B at various concentrations.

Concentration (mg L^{-1})	pH
50	4.57
300	4.28
500	4.07
1000	3.88

Effect of pH on adsorption of Rhodamine B on activated carbon

In Figure 14, it shows the effect of solution pH values on the adsorption of Rhodamine B on all of the activated carbons. Rhodamine B displays a general trend of slightly increased adsorption on all the activated carbons with the increase of solution pH values. At pH higher than 2, the adsorption amount of Rhodamine B on CAC and PrAC slightly increased with the increase of solution pH values. In addition, at low pH there is competition for the surface sited of activated carbon between protonation (H^+ adsorption on the carbon surface) and adsorption of Rhodamine B. Since the surface of CAC and PrAC are negative at pH > pH_{pzc} (3.5) and pH > pH_{pzc} (6.5) for PrAC. When pH of solution increase with increasing amount of adsorbed because the increase of solution pH values, the electrical repulsion force become weaker and the Rhodamine B may be transported to the surface of the activated carbons and become to attach on the surface due to the action of other factors such as less competitive from protonation.

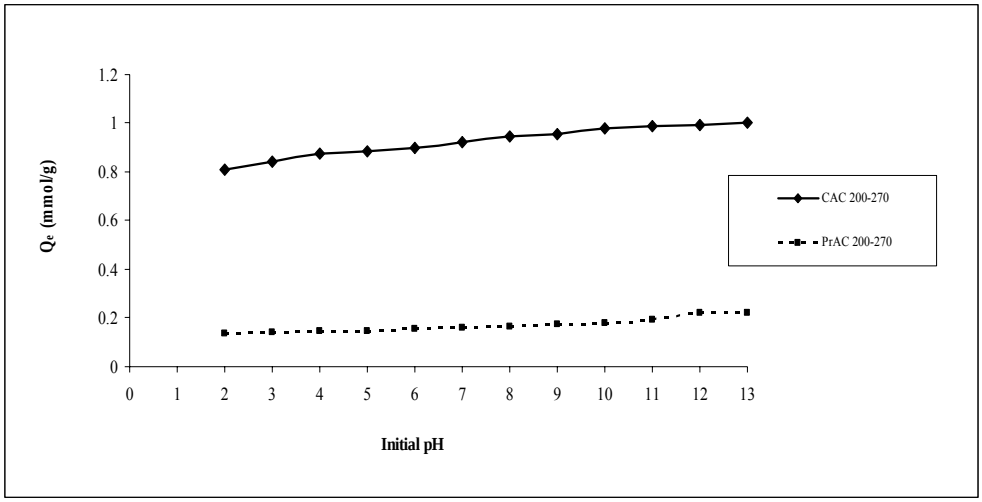

Figure 14 Adsorption of Rhodamine B on CAC (a) and PrAC (b) with pH range 2 – 13 and dye concentration 300 mg L^{-1}.

3.2.3.4 Effect of temperature

The adsorption capacity of the adsorbent increased with increase in the temperature of the system from 30 - 60 °C as shown in Table 3 and 4 for CAC and PrAC, respectively. The percentage of adsorption increases with increasing the temperature. It indicates that the adsorption process is endothermic.

Table 3 Equilibrium parameters for the adsorption of Rhodamine B 0.3 – 0.8 mmol L^{-1} on CAC 0.02 g.

C_0 (mmol L^{-1})	Temperature (°C)							
	C_e (mmol L^{-1})				% dye adsorbed			
	30	40	50	60	30	40	50	60
0.3	0.0954	0.0885	0.0806	0.0619	68	72	74	80
0.4	0.1271	0.1180	0.1137	0.0979	68	71	73	76
0.5	0.2113	0.1785	0.1734	0.1705	58	66	67	67
0.6	0.2952	0.2828	0.2684	0.2562	53	55	57	59
0.7	0.3957	0.3742	0.3735	0.3612	46	49	49	50
0.8	0.5125	0.4893	0.4757	0.4505	39	41	43	46

Table 4 Equilibrium parameters for the adsorption of Rhodamine B 0.3 – 0.8 mmol L^{-1} onto PrAC 0.09 g.

C_0 (mmol L^{-1})	Temperature (°C)							
	C_e (mmol L^{-1})				% dye adsorbed			
	30	**40**	**50**	**60**	**30**	**40**	**50**	**60**
0.3	0.0655	0.0568	0.0295	0.0273	78	82	90	91
0.4	0.1043	0.0907	0.0756	0.0633	75	78	82	85
0.5	0.1619	0.1504	0.1216	0.1065	69	71	77	79
0.6	0.2411	0.2274	0.1835	0.1432	61	64	71	77
0.7	0.3576	0.3526	0.2864	0.2080	51	52	61	72
0.8	0.4512	0.4332	0.3699	0.3476	46	48	56	58

3.2.4 Adsorption isotherm studies of Rhodamine B on activated carbons

The adsorption of Rhodamine B onto the CAC and PrAC were studied in order to assess the time required for equilibrium to be achieved. In most adsorption studies, the results showed that equilibrium was achieved within around 6 h and 24 h for CAC and PrAC, respectively. However, the solutions were left for 12 h and 30 h for CAC and PrAC, respectively, to ensure complete equilibration.

According to the Langmuir equation the equilibrium concentration of dye over the adsorbed amounts of dye (C_e/Q_e, g L^{-1}) were plotted against the equilibrium concentrations of dye (C_e) at various temperatures as shown in Figure 15 for CAC and Figure 16 for PrAC. For each temperature the graph was fitted to a straight line. Then the maximum amount of dye adsorption, Q_m (mmol g^{-1}) was calculated from the slope (= $1/Q_m$) and equilibrium constant related to the heat of adsorption, b (L $mmol^{-1}$) was calculated from the intercept (=$1/(bQ_m)$). The values of Q_m and b including the correlation coefficients, R^2, are tabulated in Table 5

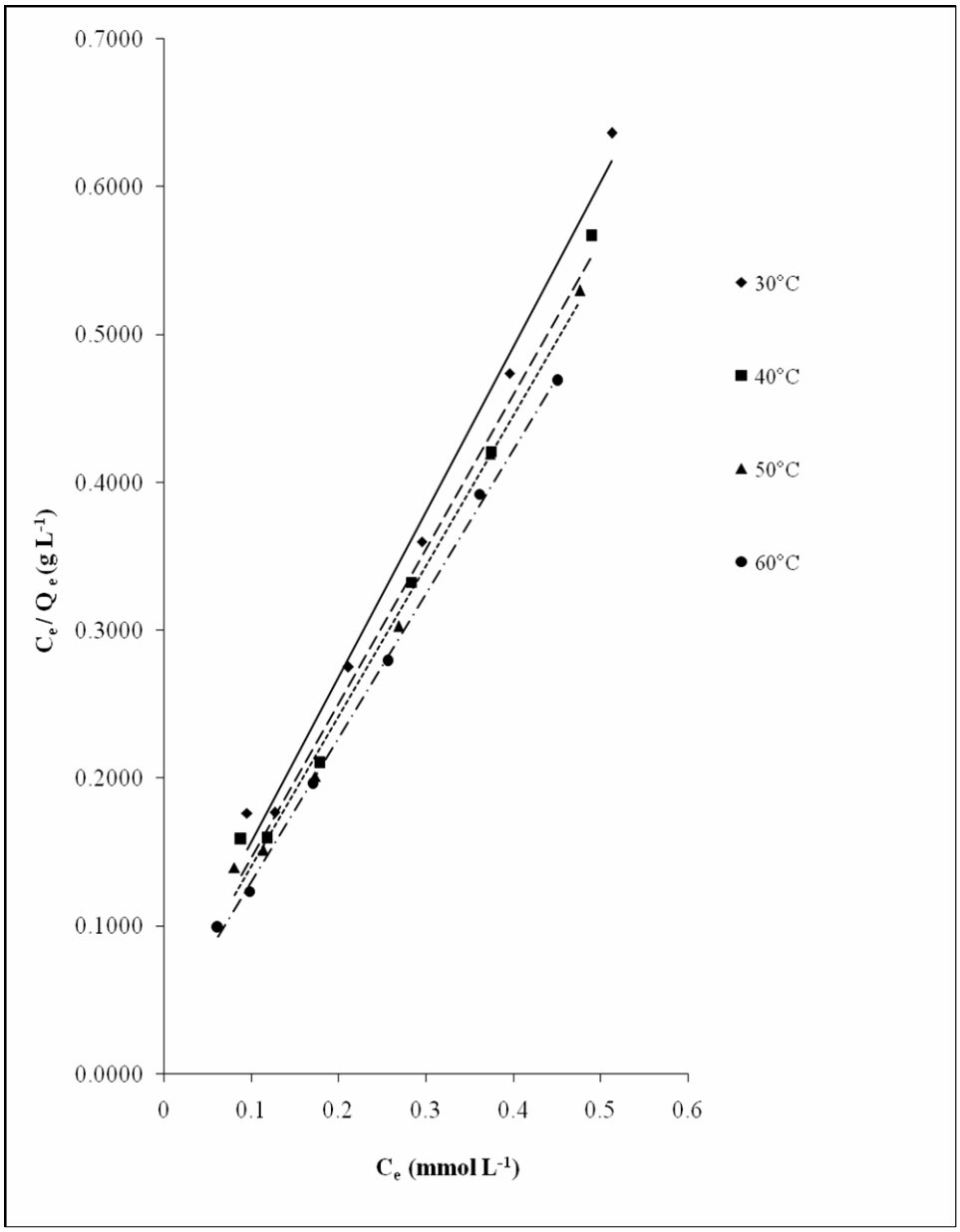

Figure 15 Langmuir adsorption isotherm for linear form of Rhodamine B on CAC (0.02 g) at 30 ºC, 40 ºC, 50 ºC and 60 ºC, dye concentrations 150 – 400 mg L^{-1} and pH = 4.

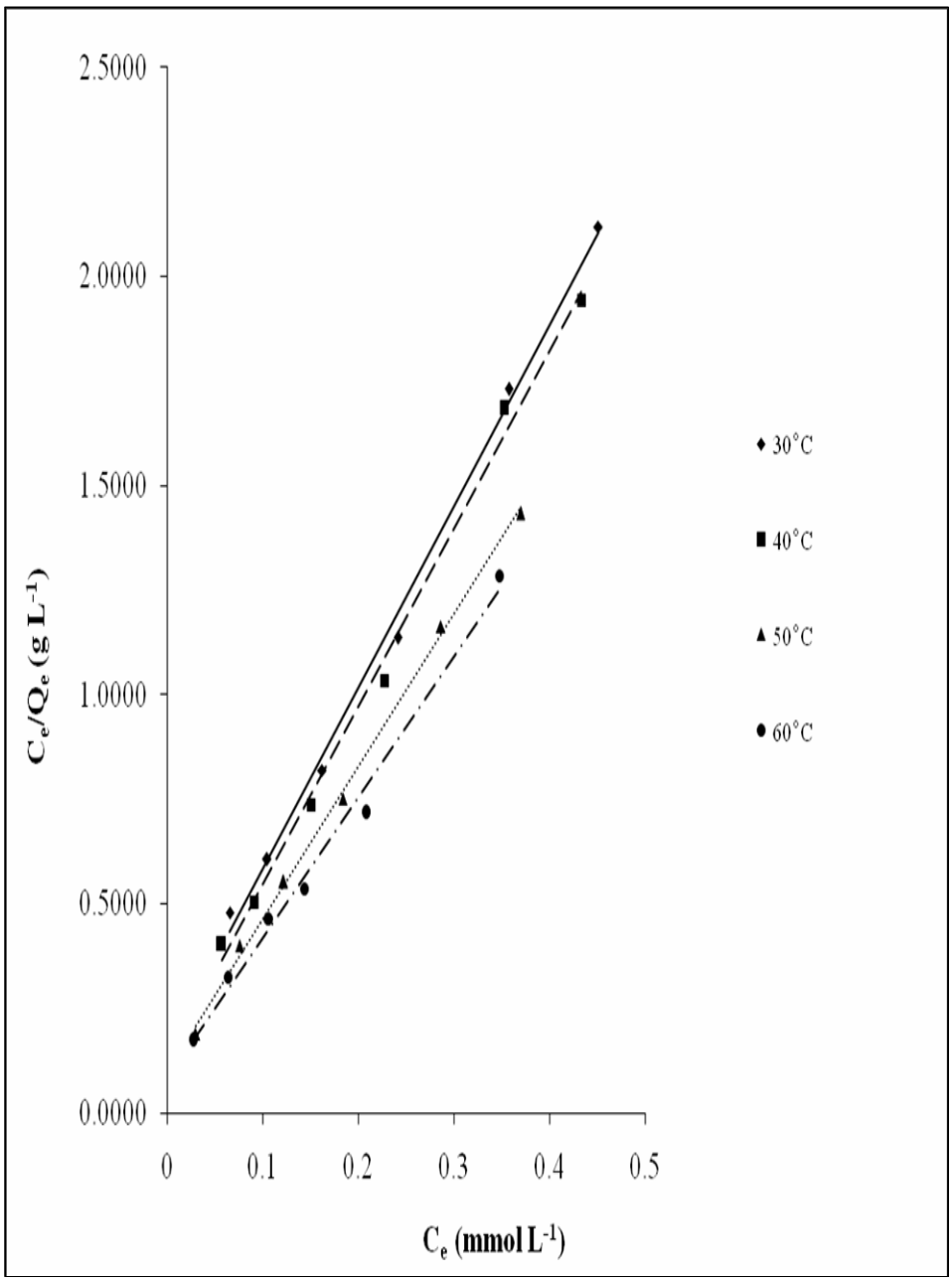

Figure 16 Langmuir adsorption isotherm for linear form of Rhodamine B on PrAC (0.09 g) at 30 ºC, 40 ºC, 50 ºC and 60 ºC, dye concentrations 150 – 400 mg L^{-1} and pH = 4.

Table 5 Parameter values of the Langmuir equations for linear form fitted to the experiment of Rhodamine B adsorption on CAC and solution PrAC at different temperatures.

AC / Temp (°C)	CAC			PrAC		
	Q_m (mmol g^{-1})	**b (L $mmol^{-1}$)**	**R^2**	**Q_m (mmol g^{-1})**	**b (L $mmol^{-1}$)**	**R^2**
30	0.90	24.76	0.9908	0.23	29.09	0.9964
40	0.96	24.95	0.9903	0.24	34.56	0.9953
50	0.98	25.99	0.9944	0.28	35.19	0.9982
60	1.03	29.71	0.9988	0.30	40.57	0.9902

The weight of CAC was 0.02 g and the weight of PrAC was 0.09 g. Those adsorption data were also fitted with the non-linear form of Langmuir equation by plotting the adsorbed amount of dye, Q_e (mmol g^{-1}) against the equilibrium concentration of dye, C_e (mmol L^{-1}) as shown in Figure 17 and Figure 18.

(a)

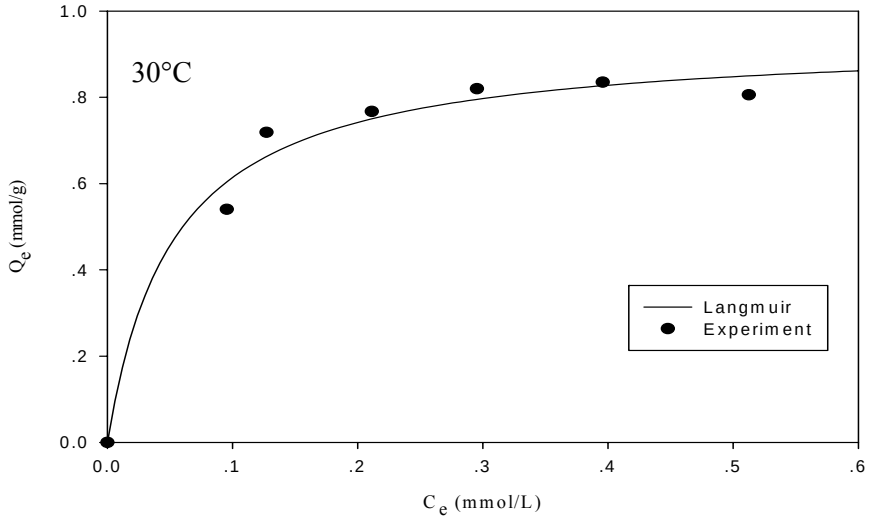
30°C
Langmuir
Experiment
Q_e (mmol/g)
C_e (mmol/L)
0.0
.2
.4
.6
.8
1.0
0.0
.1
.2
.3
.4
.5
.6

(b)

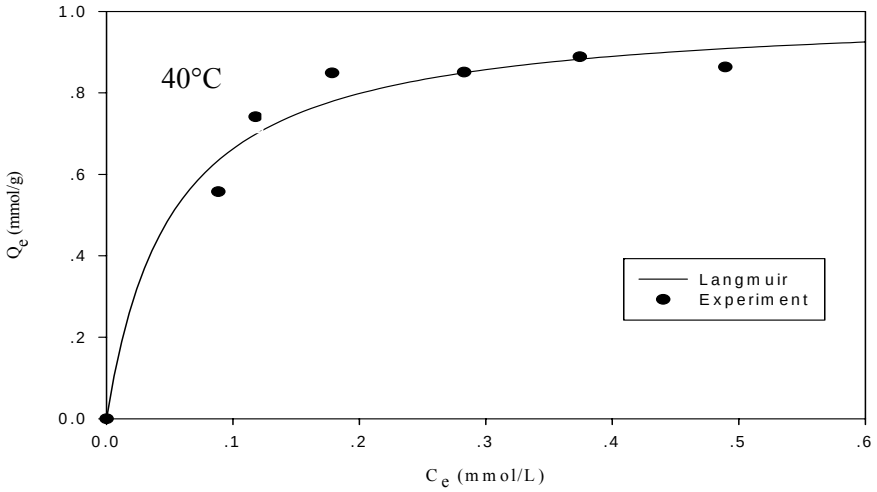
40°C
Langmuir
Experiment
Q_e (mmol/g)
C_e (mmol/L)
0.0
.2
.4
.6
.8
1.0
0.0
.1
.2
.3
.4
.5
.6

(c)

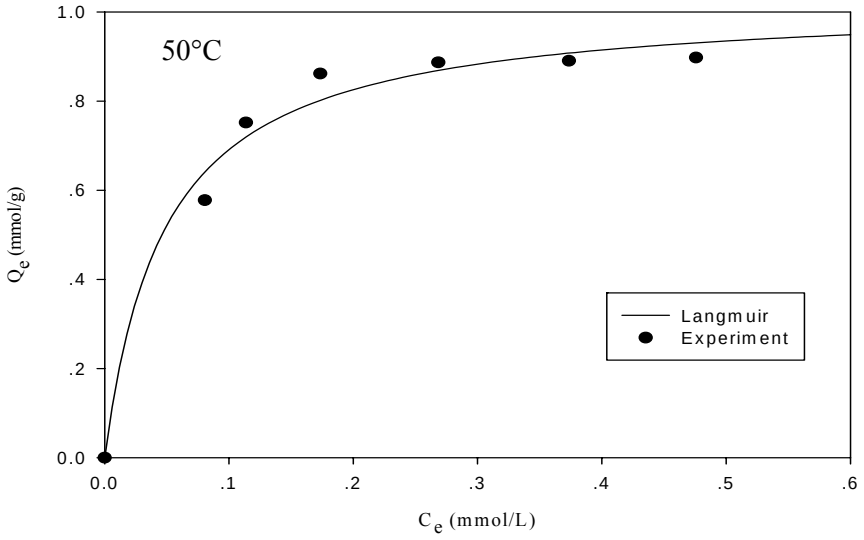
50°C
Langmuir
Experiment
Q_e (mmol/g)
C_e (mmol/L)
0.0
.2
.4
.6
.8
1.0
0.0
.1
.2
.3
.4
.5
.6

(d)

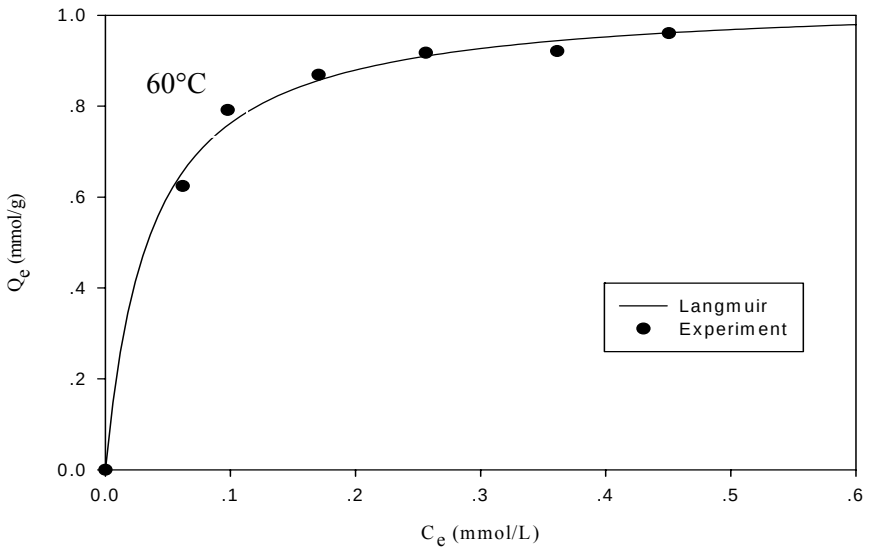

Figure 17 Langmuir adsorption isotherms for non-linear form of Rhodamine B on CAC (0.02 g) at different temperatures (a) 30 ºC (b) 40 ºC (c) 50 ºC and (d) 60 ºC, dye concentrations 150 – 400 mg L^{-1} and pH =4.

(a)

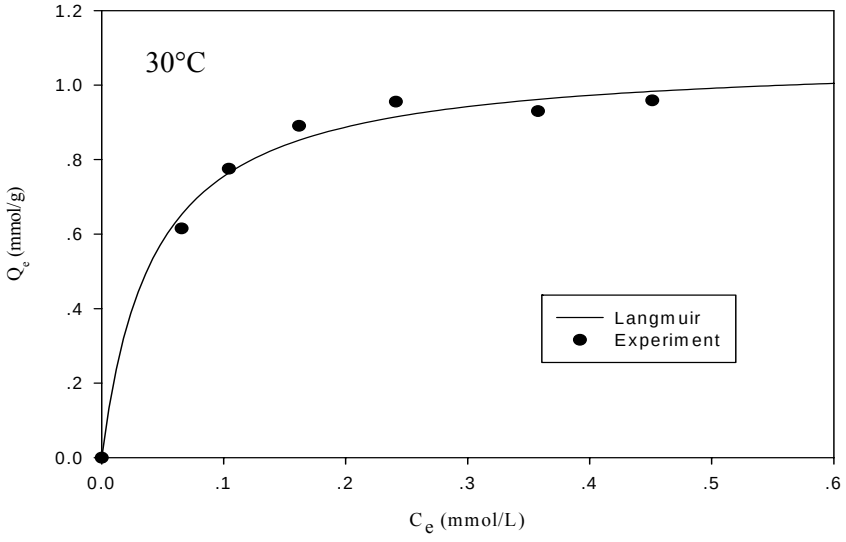

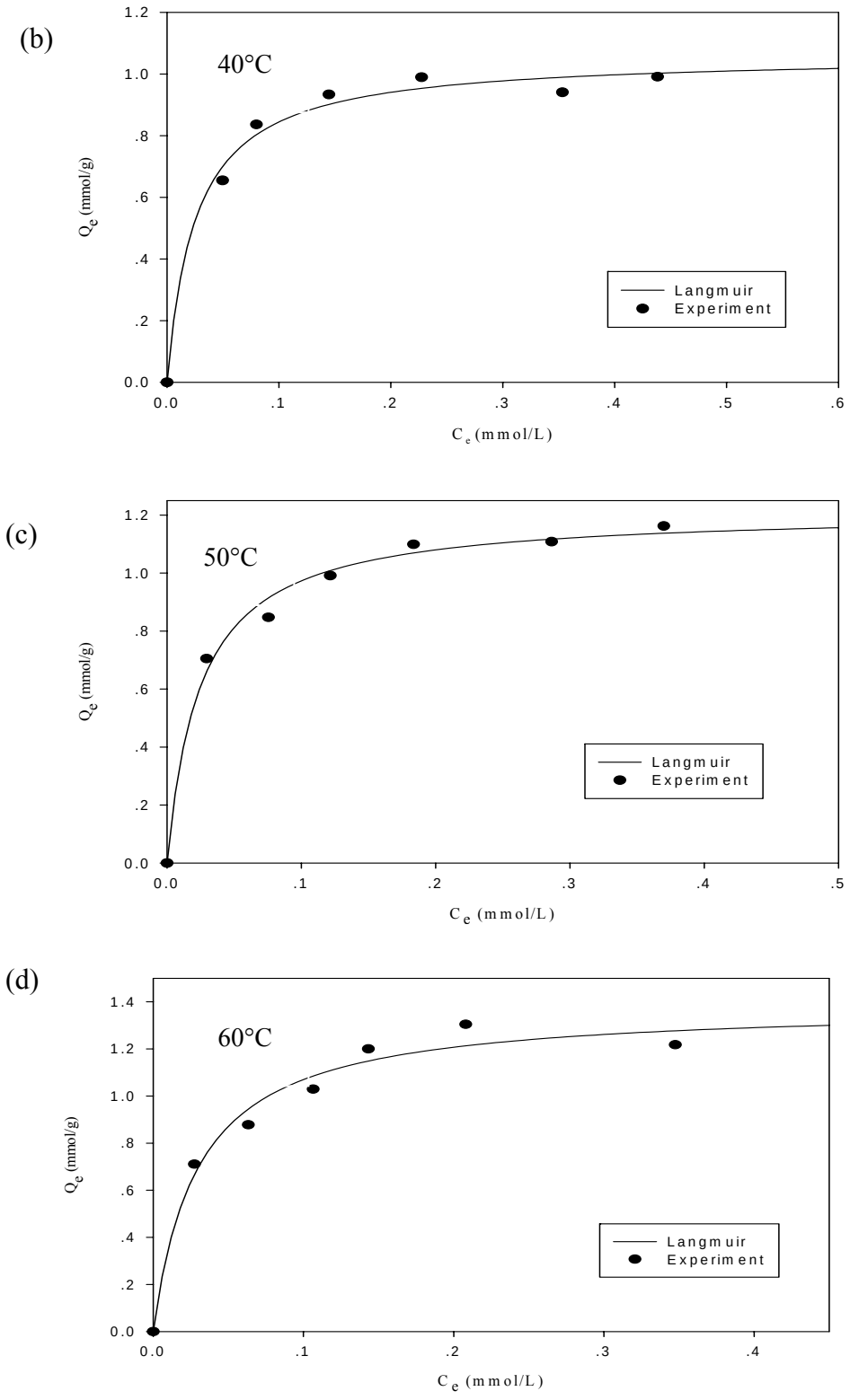

Figure 18 Langmuir adsorption isotherms for non-linear form of Rhodamine B on PrAC (0.09 g) at different temperatures (a) 30 ºC (b) 40 ºC (c) 50 ºC and (d) 60 ºC, dye concentrations 150 – 400 mg L^{-1} and pH = 4.

The values of Q_m, b and R^2 calculated from the non-linear form of Langmuir equation are tabulated in Table 6.

Table 6 Parameter values of the Langmuir equations for non-linear form fitted to the experiment of Rhodamine B (150 – 400 mg L^{-1}) on CAC (0.02 g) and PrAC (0.09 g) at different temperatures.

AC / Temp (°C)	CAC			PrAC		
	Q_m (mmol g^{-1})	**b (L $mmol^{-1}$)**	**R^2**	**Q_m (mmol g^{-1})**	**b (L $mmol^{-1}$)**	**R^2**
30	0.94	19.01	0.9813	0.25	25.53	0.9913
40	1.00	19.38	0.9762	0.26	35.91	0.9896
50	1.03	20.66	0.9839	0.29	37.49	0.9915
60	1.04	27.62	0.9959	0.31	41.90	0.9803

Figures 15 – 18 show that adsorption capacities of CAC for Rhodamine B are greater than PrAC at pH = 4 and 30 ºC, 40 ºC, 50 ºC, and 60 ºC. We can imagine that in the case of the high ionic radius of Rhodamine B, the result may be explained in terms of pore accessibility (Kadirvalu, et al., 2000). Since PrAC has micropore more than CAC, some micropore entrances may be blocked by hydrolyzed dyes species which are larger than the dye ions. Accordingly, surface groups located in micropores are no longer accessible and some surface sites are not used for adsorption. In the case of CAC which contain more mesopores, accessibility to micro- and mesopores is not blocked by hydrolyzed species and almost surface sites can be used for adsorption of Rhodamine B. In addition, acidity of surface becomes another factor to define adsorption capacities (Ferro-Garcy, et al., 1998). CAC which has lower pH_{pzc} values should have more adsorption capacities than PrAC. Therefore, it is unequivocal to

support the CAC higher adsorption Rhodamine B than on PrAC because CAC has the higher mesopore and lower pH_{pzc} value.

To confirm the favorability of the adsorption process, the dimentionless separation factor (R_L) was presented in Table 7 for CAC and Table 8 for PrAC and calculated by the following equation: (Arivoli, et al., 2007).

$$R_L \quad \frac{1}{1 \quad bC_0} \qquad (12)$$

Where R_L is dimensionless separation factor, b is an equilibrium constant related to the heat of adsorption and C_0 is the initial dye concentration.

The R_L values were found between 0 and 1 confirms the ongoing adsorption process is much more favorable (Arivoli, et al., 2007).

Table 7 Dimensionless separation factor (R_L) of Rhodamine B adsorption on CAC at different temperatures.

R_L / C_0(mg L^{-1})	Temperature(°C)			
	30	**40**	**50**	**60**
150	0.1148	0.1140	0.1099	0.0975
200	0.0888	0.0882	0.0849	0.0751
250	0.0723	0.0718	0.0691	0.0610
300	0.0609	0.0604	0.0582	0.0512
350	0.0524	0.0521	0.0501	0.0441
400	0.0462	0.0458	0.0441	0.0388

Table 8 Dimensionless separation factor (R_L) of Rhodamine B adsorption on PrAC at different temperatures.

R_L / C_0(mg L^{-1})	Temperature(°C)			
	30	**40**	**50**	**60**
150	0.0994	0.0850	0.0836	0.0733
200	0.0766	0.0653	0.0642	0.0561
250	0.0622	0.0529	0.0520	0.0454
300	0.0523	0.0444	0.0436	0.0380
350	0.0450	0.0381	0.0375	0.0327
400	0.0396	0.0335	0.0329	0.0287

From knowledge of Freundlich equation, it is expected to employ this equation for considering behavior of adsorption isotherm. According to the Freundlich equation the adsorbed amounts of dye at equilibrium (log $Q_{e,}$) were plotted against the equilibrium concentrations of dye (log C_e) at various temperatures as shown in Figure 19 for CAC and Figure 20 for PrAC. For each temperature the graph was fitted to a straight line.

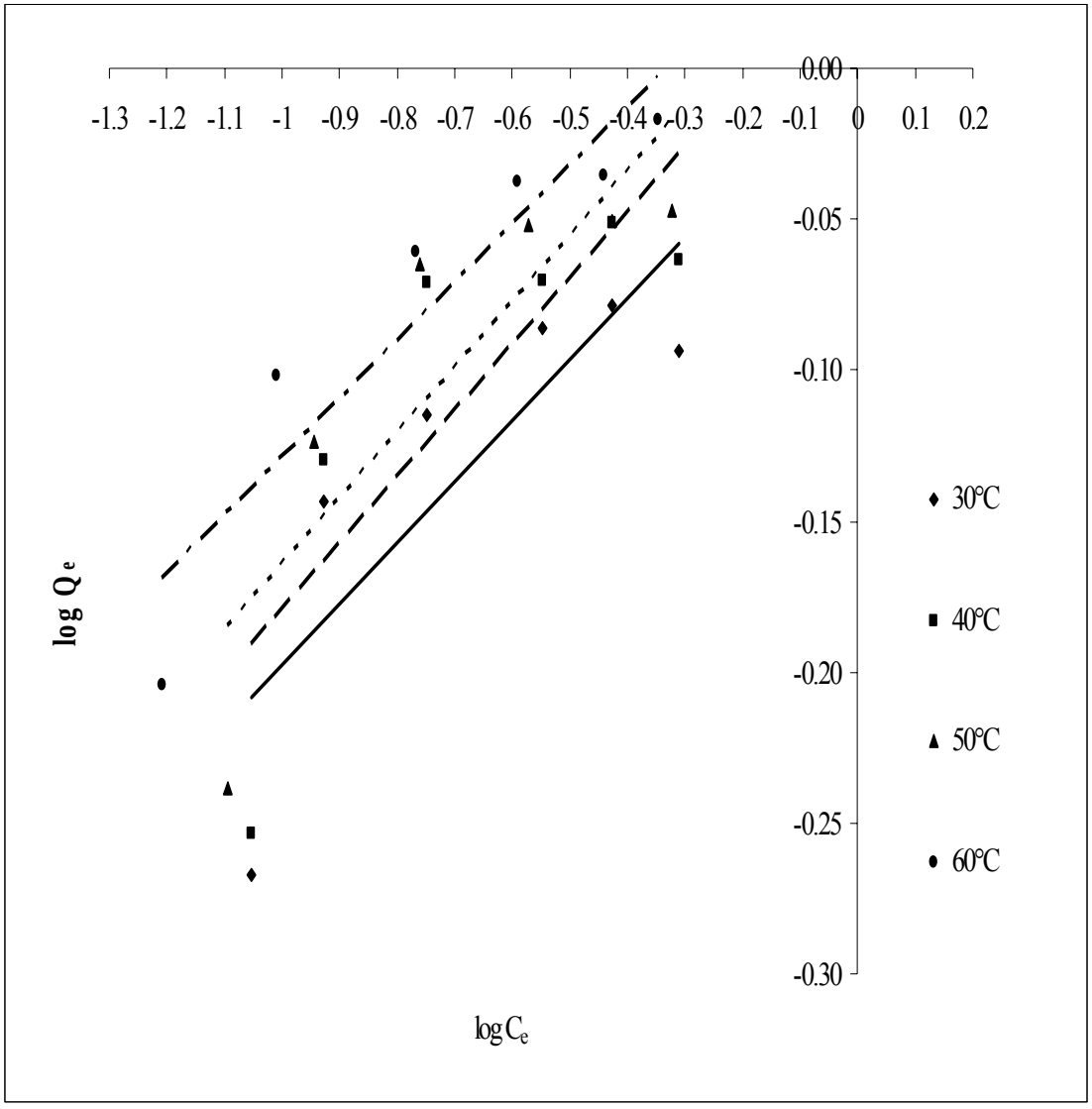

Figure 19 Freundlich adsorption isotherms for linear form of Rhodamine B on CAC (0.02 g) at different temperatures (a) 30 ºC (b) 40 ºC (c) 50 ºC and (d) 60 ºC, dye concentrations 150 – 400 mg L^{-1} and pH = 4.

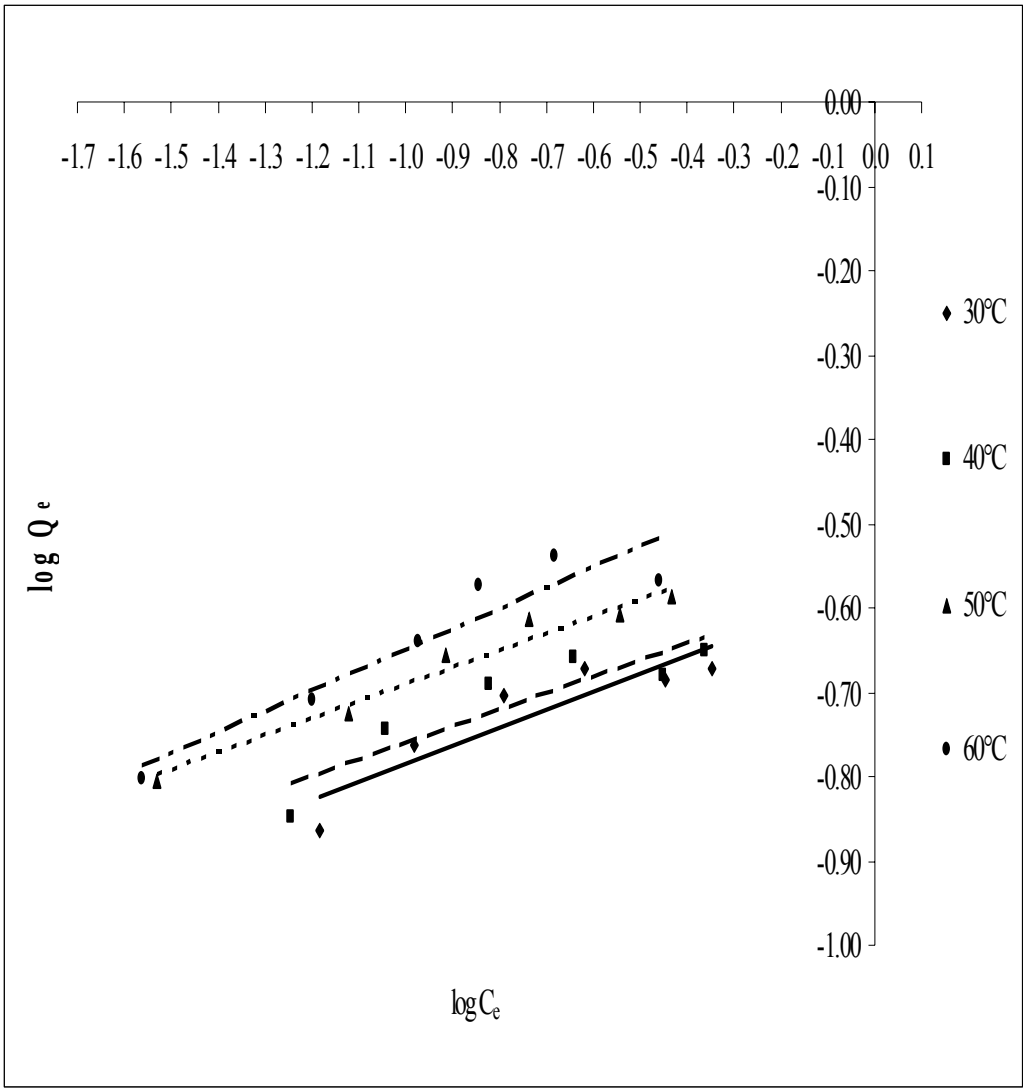

Figure 20 Freundlich adsorption isotherms for linear form of Rhodamine B on PrAC (0.09 g) at different temperatures (a) 30 ºC (b) 40 ºC (c) 50 ºC and (d) 60 ºC, dye concentrations 150 – 400 mg L^{-1} and pH = 4.

Adsorption isotherms

The adsorption data of Rhodamine B on CAC and PrAC are fitted with Langmuir isotherm both in linear and non-linear forms as shown in Figure 15 – 16 and Figure 17 – 18, respectively and the adsorption data of Rhodamine B on CAC and PrAC are fitted with Freundlich isotherm in linear form as shown in Figure 19 and 20, respectively. In Figures 19 and 20 indicated the correlation coefficient (R^2) for Freundlich equation is not approaches 1. Thus, another alternative use the Langmuir equation to explain adsorption isotherm.

Adsorption characteristics between the CAC and PrAC with Rhodamine B can be described by adsorption isotherms. In this work, the Langmuir isotherm has been used for studying the adsorption data.These isotherms relate amounts of Rhodamine B per unit weight of adsorbents (Q_e, mmol g^{-1}) to the equilibrium concentration of Rhodamine B (C_e, mmol L^{-1}). The Langmuir parameter is obtained by using nonlinear regression by fitting the data directly to the equation (1), since algebraic transformation to linear forms (equation (2) can negatively influence the estimated constants. The values of parameter of Langmuir equation for CAC and PrAC are summarized in Table 5 and Table 6, respectively. Also, to compare the reliability of these adsorption isotherms, the correlation coefficient (R^2) for each adsorption isotherm has been calculated and shown together with Langmuir parameter. The correlation coefficient (R^2) is a good criteria and means that the difference between experimental data and theoretical values is small when the values of the coefficient approaches 1 (Bembnowska, et al., 2003). The values of R^2 form linear fitting are greater than the values form non-linear fitting so linear fitting is better than non-linear fitting.

It appears that the adsorption isotherm results of both activated carbons, CAC and PrAC can be well described by the Langmuir equation but PrAC gave a slightly better fit than CAC based on the values of the correlation coefficient (R^2) for the different isotherm plots. Because of this, it is apparent that most of adsorption behavior of Rhodamine B on CAC and PrAC will be monolayer adsorption.

3.2.5 Thermodynamic considerations

From the previous study, some general conclusions can be deduced regarding the energetic changes occurring during the process. Therefore, the b parameter from Langmuir equation can be related to the enthalpy or heat of adsorption (ΔH_{ads}) as follows (Adamson and Gast, 1997)

$$b \quad b' e^{H_{ads} / RT} \tag{3}$$

Where R is the universal gas constant (8.314 J K^{-1} mol^{-1}), T is the temperature in Kelvin and b' is pre-exponential factor constant. The heat of the adsorption (H_{ads}) processat monolayer coverage can be investigated from equation if the isotherm of adsorption can be fitted with Langmuir model adequately. The heat of adsorption (H_{ads}) can be determined from slope of the observed linearity from the plot of ln b versus 1/T that leads to heat process involved in adsorption at monolayer coverage.

The correlation coefficient (R^2) for each heat of adsorption has been calculated with equation (3). However, the correlation coefficient (R^2) is not approaches 1. Thus, another alternative use the Clausius-Clapeyron equation (10) to explain heat of adsorption. Adsorption data obtained at different temperatures are used to estimate the isosteric heat of the process. The heat of adsorption was calculated by applying the Clausius-Clapeyron equation to the adsorption isotherm as follows (Alberty and Silbey, 1992 and Sirichote, et al., 2002)

$$\ln C_e \qquad \frac{H_{ads}}{RT} \quad c \tag{10}$$

Where C_e is the equilibrium concentrations (mmol L^{-1}), H_{ads} is the isosteric heat of adsorption (kJ mol^{-1}), R is the universal gas constant (8.314 J K^{-1} mol^{-1}), and c is the integration constant. Plot of ln C_e versus 1/T should give a straight line of slope - (ΔH_{ads} /R). The Clausius-Clapeyron plots of ln C_e versus 1/T of Rhodamine B on CAC and PrAC are show in Figure 21 and 22, respectively. The values of R^2 from Clausius-Clapeyron equation are greater than the values from equation (3) fitting and approaches 1 so Clausius-Clapeyron equation is better than equation (3).

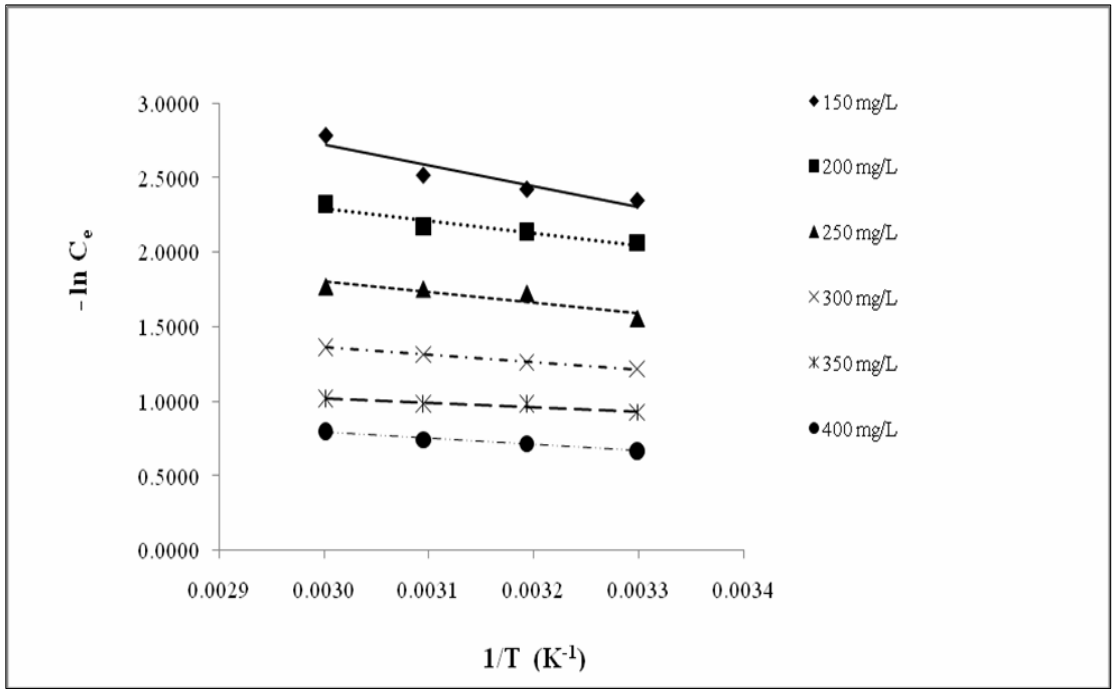

Figure 21 Clausius-Clapeyron plots for adsorption of Rhodamine B on CAC at 30 ºC, 40 ºC, 50 ºC and 60 ºC, dye concentrations 150 – 400 mg L^{-1} and pH = 4.

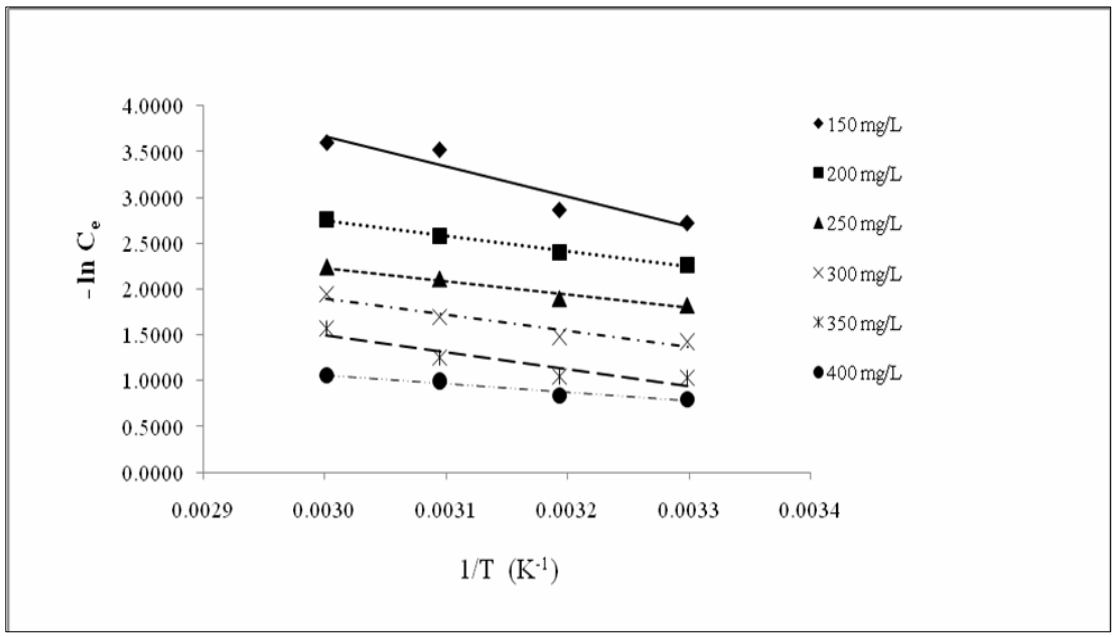

Figure 22 Clausius-Clapeyron plots for adsorption of Rhodamine B on PrAC at 30 ºC, 40 ºC, 50 ºC and 60 ºC, dye concentrations 150 – 400 mg L^{-1} and pH = 4.

Table 9 The heat of adsorption (H_{ads}) of Rhodamine B adsorption on CAC and PrAC at 30 ºC, 40 ºC, 50 ºC and 60 ºC, 150 – 400 mg L^{-1} and pH = 4.

AC / C_0 (mg L^{-1})	CAC		PrAC	
	H_{ads} (kJ mol^{-1})	R^2	H_{ads} (kJ mol^{-1})	R^2
150	11.58	0.8895	27.56	0.9001
200	6.84	0.9179	14.08	0.9931
250	5.71	0.7951	12.30	0.9648
300	4.01	0.997	14.81	0.9286
350	2.32	0.894	15.23	0.8574
400	3.48	0.984	7.88	0.9451

The positive values of the heat of adsorption (H_{ads}) from Table 9 show the endothermic nature of adsorption and H_{ads} is between 0 – 40 kJ mol^{-1} confirm that it governs the possibility of physical adsorption (Bond, 1987). Moreover, while increasing the temperature of the system, the extent of dye adsorption increases this rule out the possibility of chemisorption (Arivoli, et al., 2002).

CHAPTER 4

CONCLUSION

The commercial activated carbon (CAC) and activated carbon obtained from pericarp of rubber fruit (PrAC) were characterized for some physical properties and tested for their efficiencies in adsorption of Rhodamine B.

From SEM micrographs both CAC 200 – 270 and PrAC 200 – 270 have porous texture which are full of holes with diameters ranging around 8 – 11 μm and 4 - 20 μm, respectively. These holes are defined as macropore of the activated carbon (>50 nm). Both micropore and mesopore are not resolved by our scanning microscopy. Thus, this research has used BJH model for determining pore size distribution. Result from BJH pore size distribution show CAC remarkably has more incremental pore volume of mesopore and macropore than PrAC.

BET surface area of CAC and PrAC are 1,316.90 and 920.69 m^2 g^{-1}, respectively which indicate that both activated carbons possess a well developed porous structure. Percentages of micropore fractions of PrAC (75%) are more than the CAC (37%). Noticeably, CAC has more BET surface area than PrAC but CAC show less micropore fraction. Therefore, the physical characteristics of raw materials seem to be important factor for porous nature of activated carbon.

FT-IR spectrum of CAC is very similar to spectrum of PrAC. The strong band appears at about 3,400 cm^{-1} is mainly assigned to O-H stretching vibrations. The band observed at about 2,900 cm^{-1} which is ascribed to symmetric and asymmetric C-H stretching vibrations in aliphatic CH, CH_2 and CH_3 groups are detected. The band at about 1,600 cm^{-1} is C=C stretching vibration in aromatic ring. Many bands because of hydrogen, oxygen, and nitrogen functional groups are observed in the range 1,400 - 400 cm^{-1} which is not mentioned herein except the strong band at about 1,015 cm^{-1} can be attributed to C-O stretching vibrations.

Point of zero charge (pH_{pzc}) measurements of CAC and PrAC are 3.5 and 6.5, respectively. So the surface of CAC and PrAC are negative at pH > pH_{pzc} (3.5) and pH > pH_{pzc} (6.5) for PrAC. When pH of solution increased with increasing amount of

adsorbed because the increase of solution pH values, the electrical repulsion force become weaker and the Rhodamine B may be transported to the surfaced of the activated carbons.

The percentage of adsorption increased with increasing weight of both activated carbons. Effect of weight of activated carbon is attributed to the increase of surface area and availability of more adsorption sites. The percent adsorption decreased with increasing initial dye concentration. The adsorptions equilibrium of CAC and PrAC required 6 hours and 24 hours, respectively, for all concentrations. The percentage of adsorption increased with increasing the temperature. It confirms the endothermic nature of the process involved in the system. The maximum percentages of adsorption dye solution 150 mg L^{-1} are 80% and 91% for CAC 0.02 g and PrAC 0.09 g, at 60 $^{\circ}$C and pH 4.

The experimental data are correlated reasonably well by the Langmuir adsorption isotherm in linear and non-linear forms. The values of correlation coefficients (R^2) from the linear fitting approach to one more than the values from non-linear fitting for all temperatures. Therefore, the maximum adsorption (Q_m) obtained from linear fitting are used in the report. At 30, 40, 50 and 60°C the maximum adsorption (Q_m) for Rhodamine B on CAC are 0.90, 0.96, 0.98 and 1.03 mmol g^{-1}, respectively. And for adsorption of Rhodamine B on PrAC the maximum adsorption (Q_m) are 0.23, 0.24, 0.28 and 0.30 mmol g^{-1}, respectively. The R_L values are found to in the range between 0 and 1 which confirms that the ongoing adsorption process is much more favorable.

In thermodynamic consideration (effect of temperature), the Clausius-clapeyron equation was used to calculate the isosteric heat of adsorption of Rhodamine B because the values of correlation coefficients (R^2) from the Clausius-clapeyron equation fitting approach one better than the values from equation (3) for all temperatures. The values of heat adsorption (ΔH_{ads}) of Rhodamine B 150, 200, 250, 300, 350, 400 mg L^{-1} on CAC are 11.58, 6.84, 5.71, 4.01, 2.32, 3.49 kJ mol^{-1}, respectively. And the heat adsorptions (ΔH_{ads}) of Rhodamine B on PrAC are 27.56, 14.08, 12.30, 14.81, 15.23 and 7.88 kJ mol^{-1}, respectively. These ΔH_{ads} is between 0 – 40 kJ mol^{-1} confirm the adsorption processes to be endothermic and controlling the physical adsorption.

The efficiency of adsorption of Rhodamine B on PrAC is about 80-90%. Therefore, the agricultural product like PrAC can replace the commercial activated carbon for removal of dyes from waste water.

BIBLIOGRAPHY

Activated Carbon from Wikipedia, the free encyclopedia. http://en.wikipedia.org/wiki/Activated carbon (accessed 19/08/10)

Adamson, A. W. and Gast, A. P.1997. Physical Chemistry of Surfaces. John Wiley and Sons, Canada: 521-523.

Alberty, R.A. and Silbey, R. J. 1992. Physical Chemistry.1st Edition. John Wiley & Sons, Inc.,New York. pp. 187.

Arivoli, S. and Thenkuzhali, M. 2007. Kinetic, Mechanistic, Thermodynamic and Equilibrium Studies on The Adsorption of Rhodamine B by Acid Activated Low Cost Carbon. E-Journal of Chemistry. 5: 187-200.

Arivoli, S.; Thenkuzhali, M.; and Martin Deva Prasath, P. 2009. Adsorption of Rhodamine B by Acid Activated Carbon – Kinetic, Thermodynamic and Equilibrium Studies. Orbital the Electronic Journal of Chemistry. 1(2) : 138-155.

Barrett, E. P.; Joyner, L. G. and Halenda, P. P., 1951. Pore Size Distribution for Porous Materials. J. Am. Chem. Soc. 73: 373-380.

Bembnowska, A.; Pe-ech, R. and Milchert, E. 2003. Adsorption from Aqueous Solutions of Chlorinated Organic Compounds onto Activated Carbons. J. Colloid. Interface. Sci. 265: 276-282

Bhatnagar, A. and Jain, A.K. 2005. A Comparative Adsorption Study with Different Industrial Wastes as Adsorbents for the Removal of Cationic Dyes from Water. Journal of Colloid and Interface Science. 281: 49 -55.

Buczek, B.; Biniak, S. and S'wiatkowski, A. 1999. Oxygen Distribution within Oxidised Active Carbon Granules. Fuel. 78: 1443-1448.

Chuenchom, L. and Sirichote, O., 2004. Adsorption of Cadmium (II) and Lead (II) Ions on Activated Carbons Obtained from Bagasse and Pericarp of Rubber Fruit. Master of Science Thesis in Physical Chemistry, Prince of Songkla University.

Dye from Wikipedia, the free encyclopedia. http://en.wikipedia.org/wiki/dye (accessed 15/09/10)

Ferro-Garcy**,** M. A.; Rivera-Utrilla, J.; Bautista-Toledo, I. and Moreno-Castilla, C. 1998. Adsorption of Humic Substances on Activated Carbon from Aqueous Solutions and Their Effect on The Removal of Cr(III) Ions. Langmuir. 14: 1880-1886.

Fuente, E.; Menendez, J. A.; Dyez, M. A.; Sau'rez, D. and Montes-Moran, M. A., 2003. Infared Spectroscopy of Carbon Materials: A Quantum Chemical Study of Model Compounds. J. Phy. Chem. B. 107: 6350-6359.

Hu, Z and Vansant, E. F., 1995. A New Composite Adsorbent Produced by Chemical Activation of Elutrilithe with Zinc Chloride. J. Colloid. Interface. Sci. 176: 422-431.

Jia, Y. F.; Steele, C. J.; Hayward, I. P. and Thomas. K. M. 1998. Mechanism of Adsorption of Gold and Silver Species on Activated Carbons. Carbon. 36: 1299-1308.

Juang, R.; Wu, F. and Tseng, R., 2002. Characterization and Use of Activated Carbons Prepared from Bagasses for Liquid-Phase Adsorption. Colloid. Surface: *A*. 201: 191-199.

Kadirvalu, K.; Faur-Brasquet, C. and Le Cloirec, P. 2000. Removal of Cu(II), Pb(II), and Ni(II) by Adsorption onto Activated Carbon Cloths. Langmuir. 16: 8404-8409.

Namasivayam, C.; Muniasamy, N.; Gayathri, K.; Rani, M. and Renganathan, K. 1996. Removal of Dyes from Aqueous Solution by Cellulosic Waste Orange Peel. Biores. Technol. 57: 37.

Namasivayam, C. and Kadirvelu, K. 1999. Uptake of Mercury (II) from Wastewater by Activated Carbon from an Unwanted Agricultural Solid By-Product: Coirpith. Carbon.37: 79 – 84.

Savova, D.; Petov, N.; Yardim, M. F.; Ekinci, E.; Budinova, T.; Razvigorova, M. And Minkova. V. 2003. The Influence of The Texture and Surface Properties of Carbon Adsorbents Obtained from Biomass Products on The Adsorption of Manganese Ions from Aqueous Solution. Carbon. 41: 1897-1903.

Sirichote, O.; Innajitara, W.; Chuenchom, L.; Chunchit, D. and Naweekan, K. 2002. Adsorption of Iron (III) Ions on Activated Carbons Obtained from Bagasse, Pericarp of Rubber Fruit and Coconut Shell. Songklanakarin J. Sci. Technol. 24: 235 – 242.

Sirichote, O.; Innajitara, W.; Chuenchom, L.; Panumati, S.; Chudecha, K.; Vankhaew, P. and Choolert, V. 2008. Adsorption of Phenol from Diluted Aqueous Solutions by Activated Carbons Obtained from Bagasse, Oil Plam Shell and Pericarp of Rubber Fruit. Songklanakarin J. Sci. Technol. 30(2): 185 – 189.

Strelko, V Jr. And Malik, D. J., 2002. Characterization and Metal Sorption Properties of Oxidized Active Carbon. J. Colloid. Interface. Sci. 250: 213-220.

Vitidsant, T.; Suravattanasakul, T. and Damronglerd, S. 1999. Production of Activated Carbon from Palm-Oil Shell by Pyrolysis and Steam Activation in Fixed Bed Reactor. Science Asia. 25: 211-222.

APPENDIX

Table A1 Data of adsorption isotherm of Rhodamine B on CAC (0.02 g), pH = 4

30 °C		**40 °C**	
C_e (mmol L^{-1})	**Q_e (mmol g^{-1})**	**C_e (mmol L^{-1})**	**Q_e (mmol g^{-1})**
0.0954	0.5405	0.0885	0.5577
0.1271	0.7186	0.1180	0.7412
0.2113	0.7672	0.1785	0.8491
0.2952	0.8199	0.2828	0.8509
0.3957	0.8350	0.3742	0.8887
0.5125	0.8056	0.4893	0.8635

50 °C		**60 °C**	
C_e (mmol L^{-1})	**Q_e (mmol g^{-1})**	**C_e (mmol L^{-1})**	**Q_e (mmol g^{-1})**
0.0806	0.5775	0.0619	0.6243
0.1137	0.7520	0.0979	0.7916
0.1734	0.8617	0.1705	0.8689
0.2684	0.8869	0.2562	0.9175
0.3735	0.8905	0.3612	0.9211
0.4757	0.8977	0.4505	0.9607

Table A2 Data of adsorption isotherm of Rhodamine B on PrAC (0.09 g), pH = 4

30 °C		**40 °C**	
C_e (mmol L^{-1})	**Q_e (mmol g^{-1})**	**C_e (mmol L^{-1})**	**Q_e (mmol g^{-1})**
0.0655	0.1367	0.0568	0.1415
0.1043	0.1723	0.0907	0.1799
0.1619	0.1979	0.1504	0.2043
0.2411	0.2123	0.2274	0.2199
0.3576	0.2067	0.3526	0.2095
0.4512	0.2131	0.4332	0.2231

50 °C		**60 °C**	
C_e (mmol L^{-1})	**Q_e (mmol g^{-1})**	**C_e (mmol L^{-1})**	**Q_e (mmol g^{-1})**
0.0295	0.1567	0.0273	0.1579
0.0756	0.1883	0.0633	0.1951
0.1216	0.2203	0.1065	0.2287
0.1835	0.2443	0.1432	0.2667
0.2864	0.2463	0.2080	0.2898
0.3699	0.2583	0.3476	0.2707

VITAE

Name Miss Fareeda Hayeeye

Student ID 5110220055

Educational attainment

Degree	Name of institution	Year of graduation
Bachelor of Science (Chemistry)	Prince of Songkla University	2007

Scholarship awards during Enrollment

- Center of Excellence for Innovation in Chemistry: Postgraduate Education and Research Program in Chemistry (PERCH – CIC), Commission on Higher Education, Ministry of Education, the Department of Chemistry, and Graduate School, Prince of Songkla University.
- Teaching Assistant, Department of Chemistry, Prince of Songkla University.